DESIGN CRITERIA FOR AN EEG ALPHA-RHYTHM MONITOR

DESIGN CRITERIA FOR AN EEG ALPHA RHYTHM MONITOR

By

KENRICK IRVIN CHIN, B.ENG.

A Thesis

Submitted to the School of Graduate Studies

in Partial Fulfilment of the Requirements

for the Degree

Master of Science

McMaster University

September 1977

MASTER OF SCIENCE (1977) McMASTER UNIVERSITY
(Physics Hamilton, Ontario

TITLE: Design criteria for an EEG Alpha Rhythm Monitor

AUTHOR: Kenrick Irvin Chin, B. Eng. (McMaster University)

SUPERVISOR: Dr. T. J. Kennett

NUMBER OF PAGES: viii,63

ABSTRACT

Design criteria for construction of a device for monitoring the frequency of the alpha rhythm of the human EEG are presented in this thesis. Power spectral analysis is implemented on a minicomputer system and its limitations are illustrated. The need for a form of pattern recognition of alpha activity is revealed and satisfied subsequently by use of amplitude and duration discrimination. These techniques along with zero-crossing analysis constitute the main ideas which are recommended in the monitor design.

ACKNOWLEDGEMENTS

It is a pleasure to express my gratitude to Dr. T. J. Kennett for his guidance and encouragement and for allowing my association with the group to be such an educational and enjoyable one. I am indebted also to Dr. A.C.P. Powles of the Faculty of Medicine who initiated my interest in this research and guided me throughout this work.

I wish to specially thank Andy Robertson and Peter Brewster who were always dependable in dealing with my numerous problems, and my fellow students who made life a bit brighter.

My appreciation also goes to Mrs. Helen Kennelly for the excellent typing of the thesis.

TABLE OF CONTENTS

		Page
CHAPTER 1	INTRODUCTION	
	1.1 Introduction	1
	1.2 The Electroencephalogram and the alpha rhythm	2
	1.3 Specifications for an alpha-rhythm monitor	4
CHAPTER 2	SPECTRAL ANALYSIS	
	2.1 Spectral analysis and the Fast Fourier Transformation	5
	2.2 Proposed study	6
	2.3 Equipment	7
CHAPTER 3	RESULTS OF SPECTRAL ANALYSIS	
	3.1 Results	12
	3.2 A closer examination of spectral analysis	19
	3.3 Discussion	31
CHAPTER 4	AMPLITUDE AND DURATION DISCRIMINATION	
	4.1 Implementation	37
	4.2 Results	43
	4.3 Statistical analysis of results	45
	4.4 Conclusions	53
CHAPTER 5	ALPHA FREQUENCY MONITOR	
	Design recommendations	54
APPENDIX A	FOURIER TRANSFORMS	58
REFERENCES		62

LIST OF ILLUSTRATIONS

Figure		Page
2.1	Real-Time Analysis System	9
2.2	Nova Minicomputer System for Off-line Analysis	11
3.1	Power Spectra of 16-sec EEG Records	13
3.2	Power Spectra of 16-sec EEG Records After Frequency Smoothing	15
3.3	Power Spectra of 8-sec EEG Records	16
3.4	Power Spectra of 4-sec EEG Records	17
3.5	Power Spectra of 2-sec EEG Records	18
3.6	Sum of Two 8-sec Power Spectra	20
3.7	Sum of Four 4-sec Power Spectra	21
3.8	Sum of Eight 2-sec Power Spectra	22
3.9	Variation of Alpha Frequency with Time	23
3.10	Power Spectra of 10-Hz Sine Wave with Rectangular Window	25
3.11	Power Spectra of 10-Hz Sine Wave with Sine Windows	26
3.12	Power Spectra of Simulated Alpha Spindles at Different Size	27
3.13	Power Spectra of Simulated Alpha Spindles at Various Positions in Time	29
3.14	Power Spectra of Simulated Alpha Spindles Under Various Conditions of Phase Difference	30

Figure		Page
3.15	Power Spectrum of 8-sec Record	32
3.16	Power Spectrum of EEG Segments	33
3.17	Power Spectrum of EEG Segments	34
4.1	Power Envelope Detection	38
4.2	Distribution of Peak Values of Power Envelope	40
4.3	Application of Power Threshold	41
4.4	Application of Power and Duration Threshold	42
4.5	Distribution of Spindle Energy	46
4.6	Distribution of Time Interval Between Spindles	47
4.7	Distribution of Time Interval Between Spindles	48
4.8	(a) Distribution of Spindle Duration (b) Mean Alpha vs Duration (c) Mean Alpha vs Duration	49
5.1	Block Diagram of Proposed Monitor	55
A.1	Examples of Fourier Transforms and Convolution	61

LIST OF TABLES

Table		Page
4.1	Spindle Analysis Following Application of Power and Duration Thresholds	44
4.2	Statistics of Spindles Grouped According to Duration	50
4.3	Spindle Information	52

CHAPTER 1

INTRODUCTION

1.1 Introduction

Many attempts have been made to relate the major characteristics of the electroencephalogram (EEG) to physiological conditions. These investigations have relied heavily on the visual inspection of the EEG record by trained technicians and neurologists. With the recent advances in electronic and computer technologies, more objective, quantitative techniques have been introduced. Some of these such as spectral analysis, auto- and cross-correlation and period analysis, are well described in various publications[1-3]. It is hoped that a practical alpha-rhythm monitor which incorporates some of these recent techniques can be designed and constructed. The monitor would then be applied to clinical research on hypoxia and respiratory problems that are currently being investigated at the McMaster University Medical Centre.

The object of this research is to analyze the alpha rhythm of the EEG in order to identify and quantify the major parameters involved. Based on these results, design criteria will be recommended for the construction of a practical, low cost alpha-rhythm monitor.

1.2 The Electroencephalogram and the alpha rhythm

Electrical activity within the brain is observed in the form of surface potentials by the proper placement of electrodes on the scalp. The resulting electrical signal, known as the EEG, has been directly correlated with neurological processes and thus has become a valuable aid in the diagnosis of mental disorders.

Traditionally, the EEG is recorded on paper using special amplifiers feeding into multichannel chart recorders. Due to the nature of the EEG recording, special care is required in its execution. Standard recording procedures have therefore been developed[4]. Of particular importance is the guarding of the EEG recording from the effects of extracerebral activities which may introduce artefacts. Several common causes of artefacts are eye-movements, heart-beat, respiration, electrical interference, and faults in the recording apparatus. Electroencephalographers are therefore trained in the accepted recording procedures as well as in recognizing and minimizing artefacts.

Describing the complex shape of the EEG can be a difficult task. Classification therefore begins with the recognition of basic features. The three most commonly accepted components of the EEG are the rhythmic wave forms, the shorter lasting transients, and the background activity. The frequent occurrence of the rhythmic wave-like feature has resulted in

the EEG being described in terms of waves and spindles. A wave can be thought of as one complete cycle while a spindle or burst represents a number of waves occurring in succession. Each wave has a specific wave-length and is therefore classified according to its respective frequency (reciprocal of wave-length).

The commonly recognized bands of frequency are:

DELTA: below 4-Hz

THETA: from 4 to 8-Hz

ALPHA: from 8 to 13-Hz

BETA: above 13-Hz.

Alpha rhythm is the term used when referring to the rhythmic spindles which fall within the 8 to 13-Hz range. These alpha spindles are generally observed in the EEG taken from the posterior portion of the scalp and are most predominant when the subject is relaxed with his eyelids closed. In most adults the alpha rhythm has a mean frequency in the 9 to 10-Hz region. Generally, this frequency may vary about its mean by ±0.5 Hz in normal subjects under stable conditions[4]. It has been found that the alpha frequency is affected by various physiological conditions such as changes in concentrations of sugar, carbon dioxide, and oxygen in the blood[5]. The results of this and more recent investigations indicate that a clinical apparatus which could monitor and display the alpha frequency would be a valuable tool in both research and hospital care.

1.3 Specifications for an alpha-rhythm monitor

The main function of the monitor is to determine the mean frequency of the alpha rhythm. The result should be immediately visible though it may be automatically recorded for further study. It is foreseen that once the reliability of the monitor has been proven, it would ultimately become a bed-side monitor as well as a research instrument. Therefore it ought to be compact, portable, inexpensive, and not in need of attention of someone specifically trained in its operation. Furthermore, one should be able to set minimum and maximum limits on the alpha frequency whereby a visual and/or audible alarm would be issued by the monitor if the frequency deviated beyond the set limits.

CHAPTER 2

SPECTRAL ANALYSIS

2.1 Spectral analysis and the Fast Fourier Transformation

Spectral analysis of the EEG has advanced notably since wave counting by manual means was employed. The Fourier Transformation (FT) of a time series into its frequency components has long been regarded as the classic technique for spectral analysis. However, its implementation tended to be costly and time consuming, requiring large-scale computer systems which allowed only off-line analysis. The later development of the Fast Fourier Transformation (FFT) algorithm[6] introduced a substantial saving in the computational time required to perform the FT. This technique has now come into wide-spread use and, in conjunction with the increased availability of computer data-processing systems, has become the basis for spectral analysis in innumerable fields.

Much of the present day research on spectral analysis of the EEG still rely on off-line data analysis and therefore cannot provide immediate results to the investigator. This drawback can now be easily overcome with the use of physically small, low-cost minicomputers which are readily available. An even more attractive solution is now possible

with the advent of microprocessors and semiconductor memories which have drastically reduced the size and cost of computer systems.

2.2 Proposed study

This thesis describes the implementation of the FFT algorithm on a minicomputer system for the purpose of performing power spectral analysis of the EEG in real-time. Several graphical presentations of frequency spectra shown throughout this text give some indication of the difficulty in determining the mean alpha frequency. This difficulty which arises from the occurrence of a number of alpha peaks in the frequency spectrum was previously reported[7]. The origin of these multiple peaks will be explained with the aid of illustrated simulations of alpha spindles. It will be shown that multiple peaks can be eliminated if some form of pattern recognition of alpha spindles were applied prior to spectral analysis. The need for pattern recognition has been expressed and electronic devices aimed at accomplishing this have been reported[8,9].

Power spectral analysis using the FFT is capable of providing information spreading over a wide frequency range. Methods of tracking the mean alpha frequency over a more limited range have been proposed. Zero-crossing analysis[10] and phase-locked loop[11] are two examples which have been applied to EEG analysis. These techniques appear attractive

since either can be implemented at a much lower cost than the FFT. Later in this study, results from zero-crossing analysis will be compared with those from FFT analysis. This will eventually lead to a monitor design based on pattern recognition and zero-crossing analysis.

2.3 Equipment

The study of power spectral analysis of the EEG required the use of a system which was flexible enough to allow various modes of analysis to be performed. For this reason a system based on a minicomputer was adopted. Equipment for a more specific application need not be as complex. The design of a compact alpha-rhythm monitor is presented later in this thesis.

EEG samples used in this research were prerecorded on a frequency-modulated tape recorder. The analog signal was then band limited by a 30-Hz, 12-dB/octave, low-pass filter prior to digitization. Since on-line spectral analysis was initially the primary objective, the use of a NOVA minicomputer (Data General Corporation) with a floating-point arithmetic processor appeared to suit the requirements well. This minicomputer system consisted of 32 K of 16-bit words of magnetic core memory, a 5M-byte disk, and a Real-time Disk Operating System (RDOS). A Discrete Fourier Transformation (DFT) program capable of performing a fast Fourier transformation of an array of 1024 complex points within 2 seconds was used throughout

this research. This software package was developed and supplied by Data General Corporation.

A second minicomputer, a PDP-15 (Digital Equipment Corporation) with 8K of 18-bit words of memory was also used since it was already equipped with an analog-to-digital converter (ADC) and a graphic video-display unit. The 12-bit ADC (BURR-BROWN ADC30-12Z-BTC) had a maximum conversion time of 40 microseconds and was therefore fully capable of digitizing the much slower EEG wave-forms. A block diagram indicating the flow of data within the computer system is shown in figure 2.1.

Computer programs for both the PDP-15 and NOVA computers were written in the respective assembly language of each computer. These programs were designed in such a way that important parameters could be easily changed. The parameters considered were:

(i) sampling rate,

(ii) record length, and

(iii) horizontal and vertical scaling for the graphic display.

Alteration of other input parameters allowed various modes of analysis to be selected. These modes were:

(i) power spectral analysis with no averaging,

(ii) averaging over a number of records,

(iii) continuous time-weighted averaging, and

(iv) smoothing in the frequency domain.

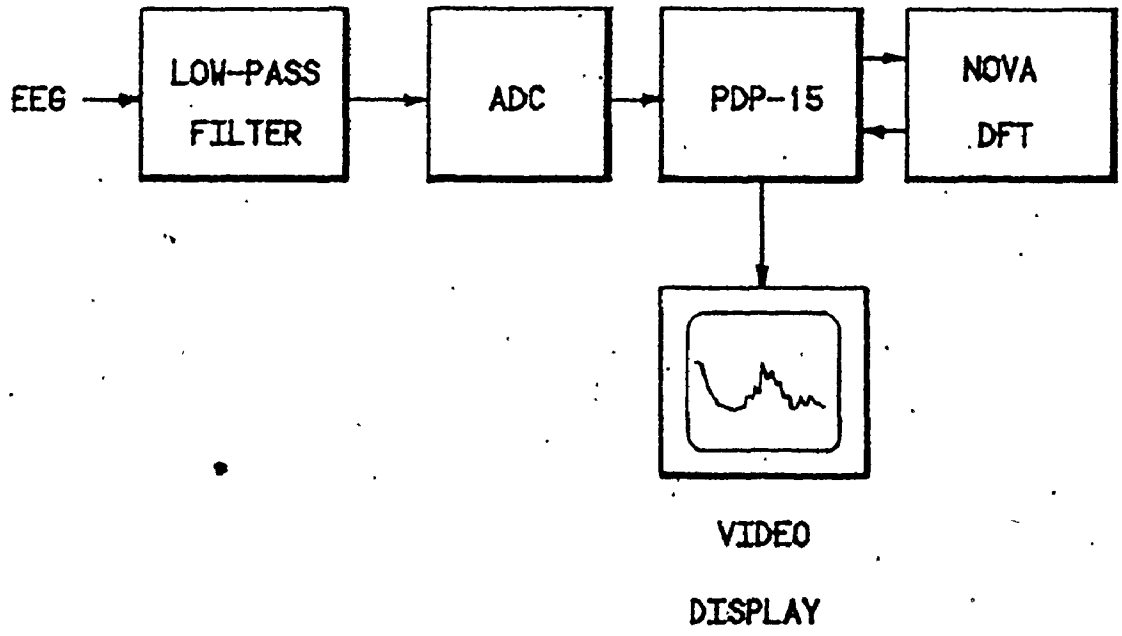

FIG. 2.1 REAL-TIME SPECTRAL ANALYSIS SYSTEM

A sampling rate of 64 Hz was selected thus providing analysis of frequencies up to 32 Hz. Since the DFT program handled a maximum array size of 1024 points, the duration of the sampled record was limited to a maximum of 16 seconds. The lower limit was set at 2 seconds when all the data handling procedures were taken into account.

The system as described above constituted a feasible on-line EEG spectrum analyser. In order to utilize such a system as a more specialized real-time EEG monitor, one would need only to implement convenient means of inputing and extracting various control and signal parameters. An immediate refinement to the system would be to eliminate one of the two processors; the function of the PDP-15 could be assumed by the NOVA computer.

Once it was demonstrated that the system could analyze and display EEG frequency spectra in real-time, the system was reorganized to facilitate a closer study of the DFT as a suitable technique for analyzing EEG records. The digitized EEG data was stored as a NOVA RDOS disk file thus allowing repeated access to the same data for comparison of different types of analysis. All subsequent analyses were performed on the NOVA computer using programs written in FORTRAN. Hard-copy graphs were made available through a strip-chart plotter which was interfaced to the NOVA. This setup is shown in figure 2.2.

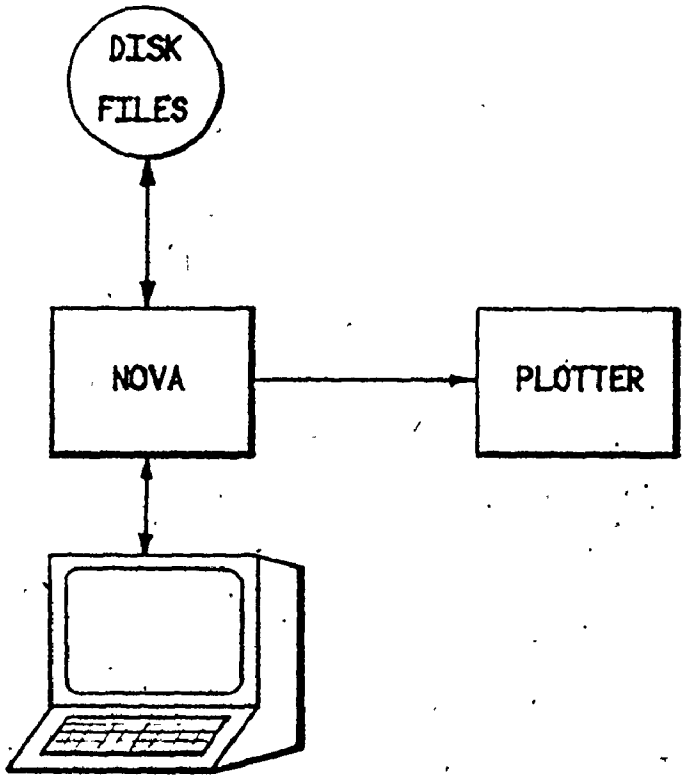

FIG. 2.2 NOVA MINICOMPUTER SYSTEM FOR OFF-LINE ANALYSIS

CHAPTER 3

RESULTS OF SPECTRAL ANALYSIS

3.1 Results

The EEG analyzed in this study consisted of recordings taken from the left parieto-occipital lobes of a normal male subject. These recordings were made while the subject was relaxed, with his eyelids closed, and not actively thinking. The first eight graphs to be shown illustrate typical results of the spectral analysis used. Figure 3.1 shows the frequency spectrum which was calculated from consecutive 16-second records. One distinct feature revealed is the fine structure of the spectrum which gives the impression that the 16-second EEG record consists of a number of alpha spindles each occurring at sharply defined frequencies. Also observable is the intermittent nature of alpha spindles in that some of the 16-second records show no activity within the 8 to 13-Hz region.

Since one objective of this analysis was to determine the mean frequency of the alpha rhythm, it appeared desirable to eliminate the fine fluctuations by smoothing the spectrum in the frequency domain. This was achieved by performing a 3-point average whereby each point in the resulting spectrum

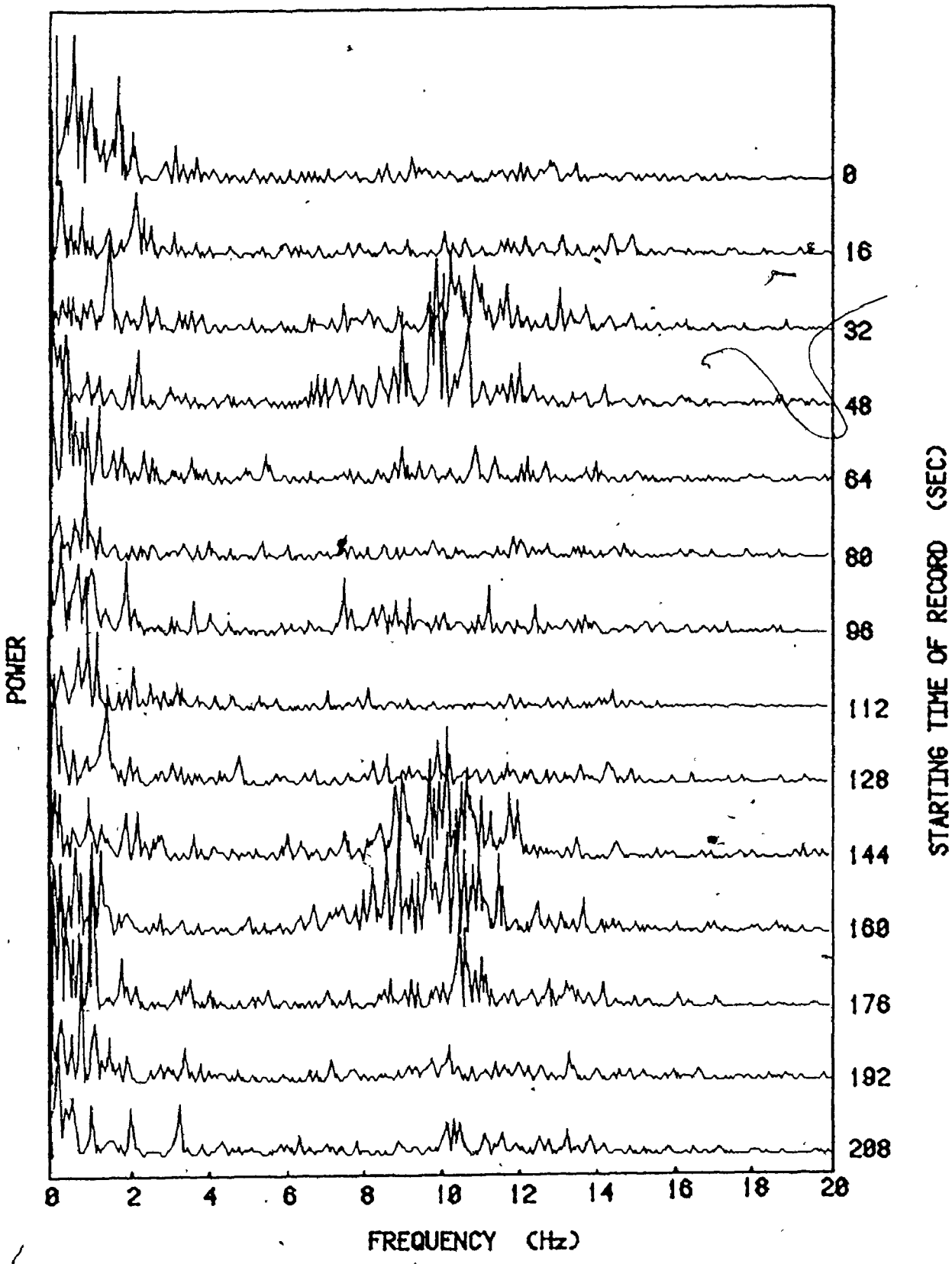

FIG. 3.1 POWER SPECTRA OF 16-SEC EEG RECORDS

was derived from the arithmetic mean of three points of the original spectrum. This procedure is equivalent to convolution (see appendix A) of a 3-point rectangle with the power spectrum. The result of this smoothing process can be seen in figure 3.2 when compared to the original spectra previously shown in figure 3.1.

In general, the smallest discernable increment on the frequency scale is given as the reciprocal of the record duration. Thus for a 16-second record the minimum frequency step is 0.06 Hz. Figures 3.2 to 3.5 show the effects of using 16, 8, 4, and 2-second record durations. The degradation of the frequency resolution can be clearly seen in light of the previous discussion. Moreover, the numerous multiple peaks observed in the power spectra of 16-second records have been averaged into almost one in the 2-second spectra. Thus the alpha peak can be more easily identified in the latter case. When the spectra of 2-second records were examined, alpha activity was observed in only some of the spectra. This finding supports the concept that the alpha rhythm consists of short bursts of alpha spindles, occurring with durations which perhaps may be even shorter than 2 seconds.

In an attempt to display an averaged representation of the alpha activity, each group of 8, 4, and 2-second results were separately summed to encompass the activity occurring over 16-second periods. The results of this procedure

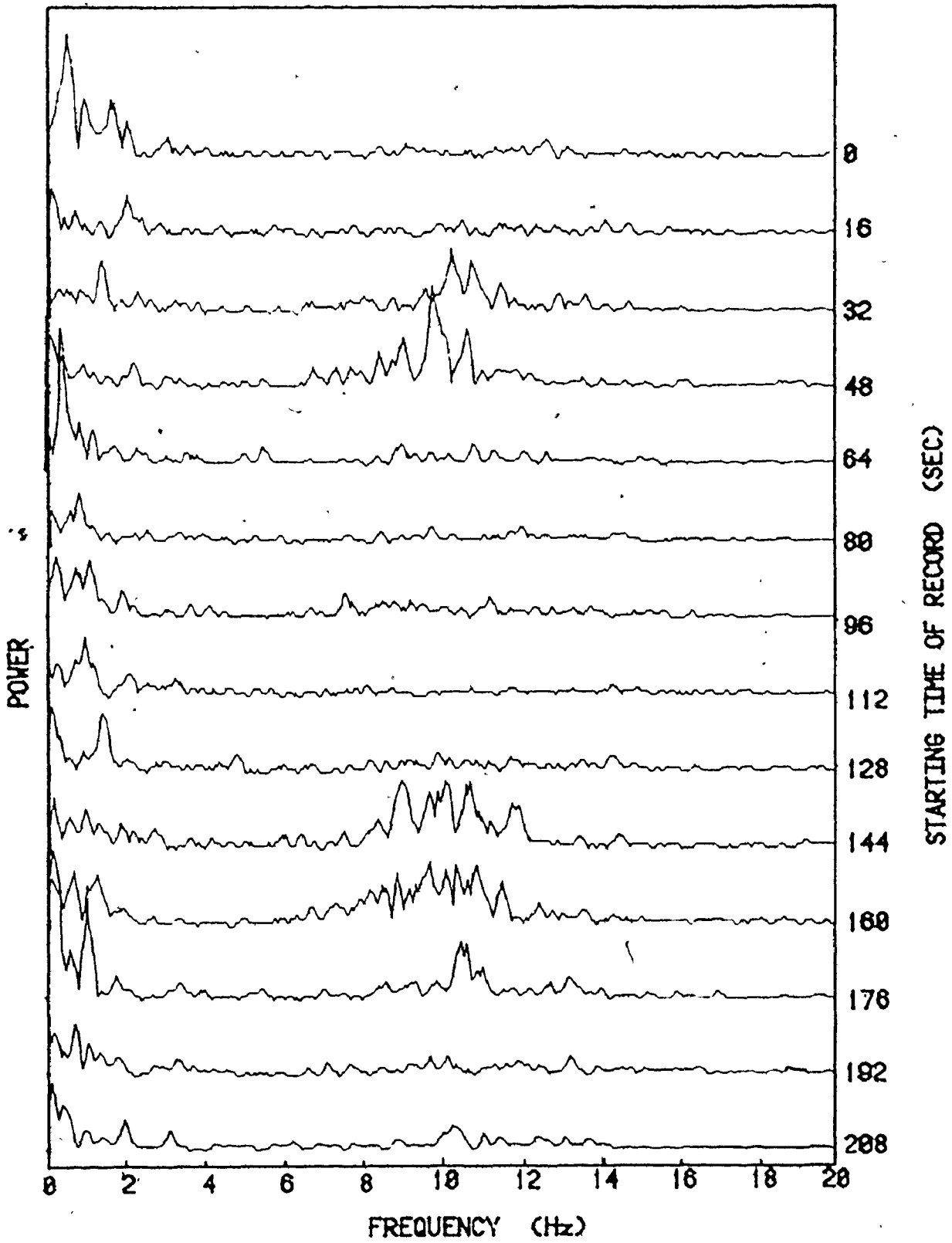

FIG. 3.2 POWER SPECTRA OF 16-SEC EEG RECORDS AFTER FREQUENCY SMOOTHING

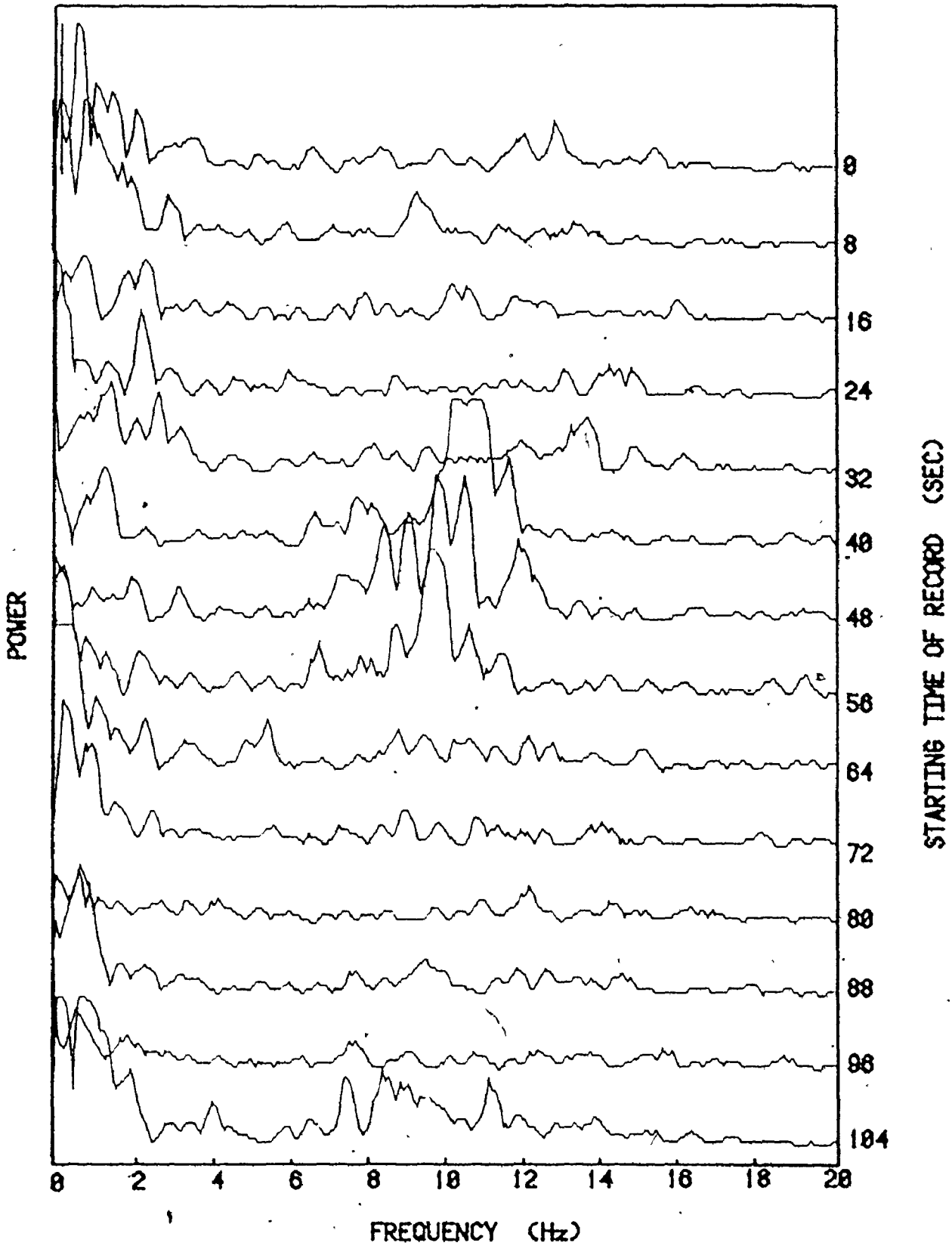

FIG. 3.3 POWER SPECTRA OF 8-SEC EEG RECORDS

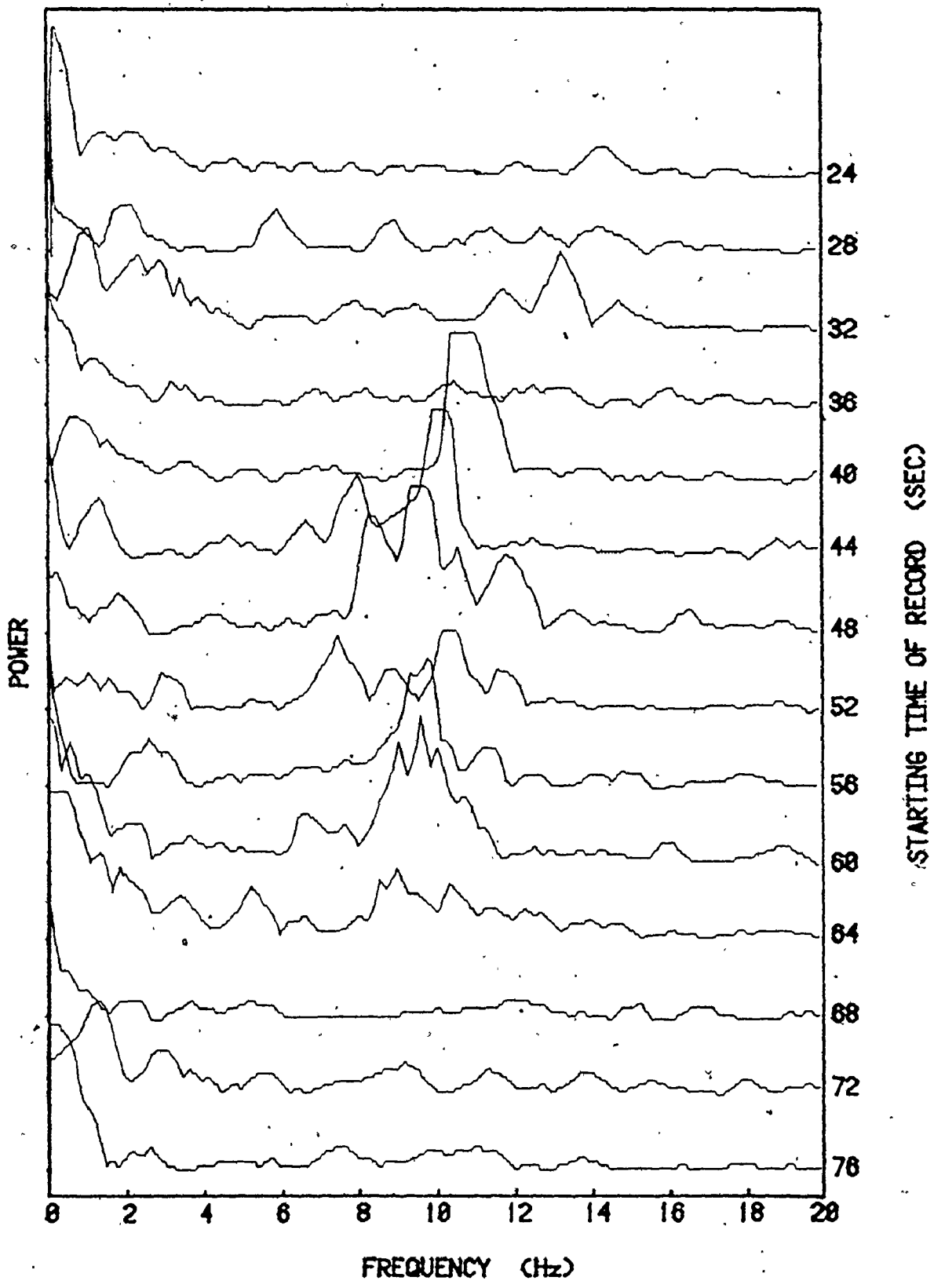

FIG. 3.4 POWER SPECTRA OF 4-SEC EEG RECORDS

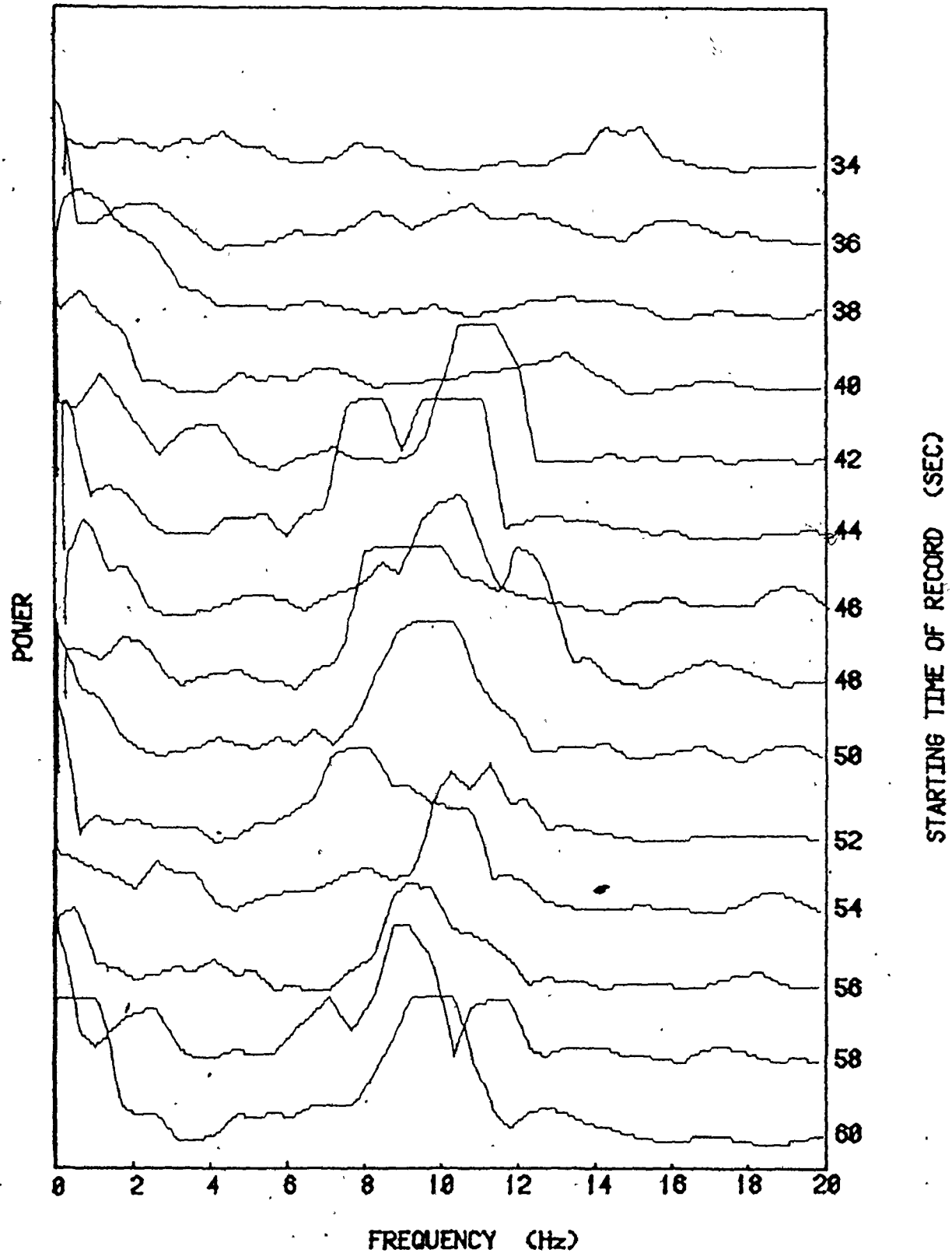

FIG. 3.5 POWER SPECTRA OF 2-SEC EEG RECORDS

as shown in figures 3.6, 3.7, and 3.8 can be compared. Because of its smoothed appearance the sum of eight 2-second records shown in figure 3.8 may be an acceptable way of presenting a less complicated view of the alpha activity.

Finally, for each of the 16, 8, 4 and 2-second results the mean alpha frequency was determined within the 8 to 13-Hz range. These results were then plotted, as shown in figure 3.9, to reveal the variation in the mean alpha frequency with time. The alpha frequency of 2-second records displayed wide fluctuations ranging from 9.5 to 11.5 Hz. When averaged over 16-second records these short-term fluctuations were substantially reduced.

3.2 A closer examination of spectral analysis

In order that a better understanding of the fine structure of the power spectrum could be obtained, the spectra of mathematical functions closely resembling alpha spindles were studied. Consequently, a number of interesting features were revealed. In the following discussion the convolution theorem is frequently mentioned. The reader who is not too familiar with this theorem should refer to appendix A where some definitions and properties of the FT are briefly presented.

The following five figures illustrate by the use of mathematical simulations, properties of the FT in relation to alpha spindles. This analysis consisted of creation of time

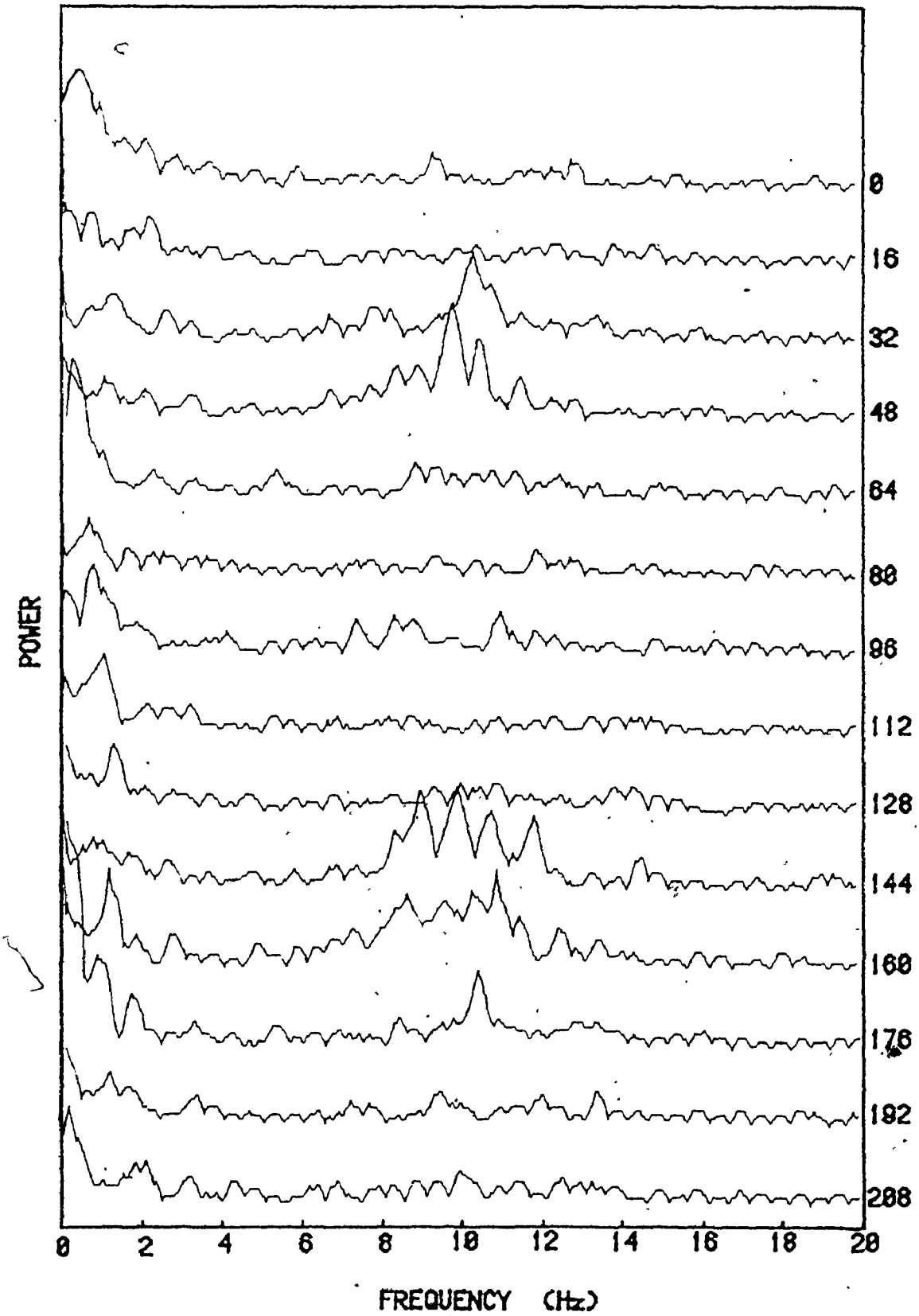

FIG. 3.6 SUM OF TWO 8-SEC POWER SPECTRA

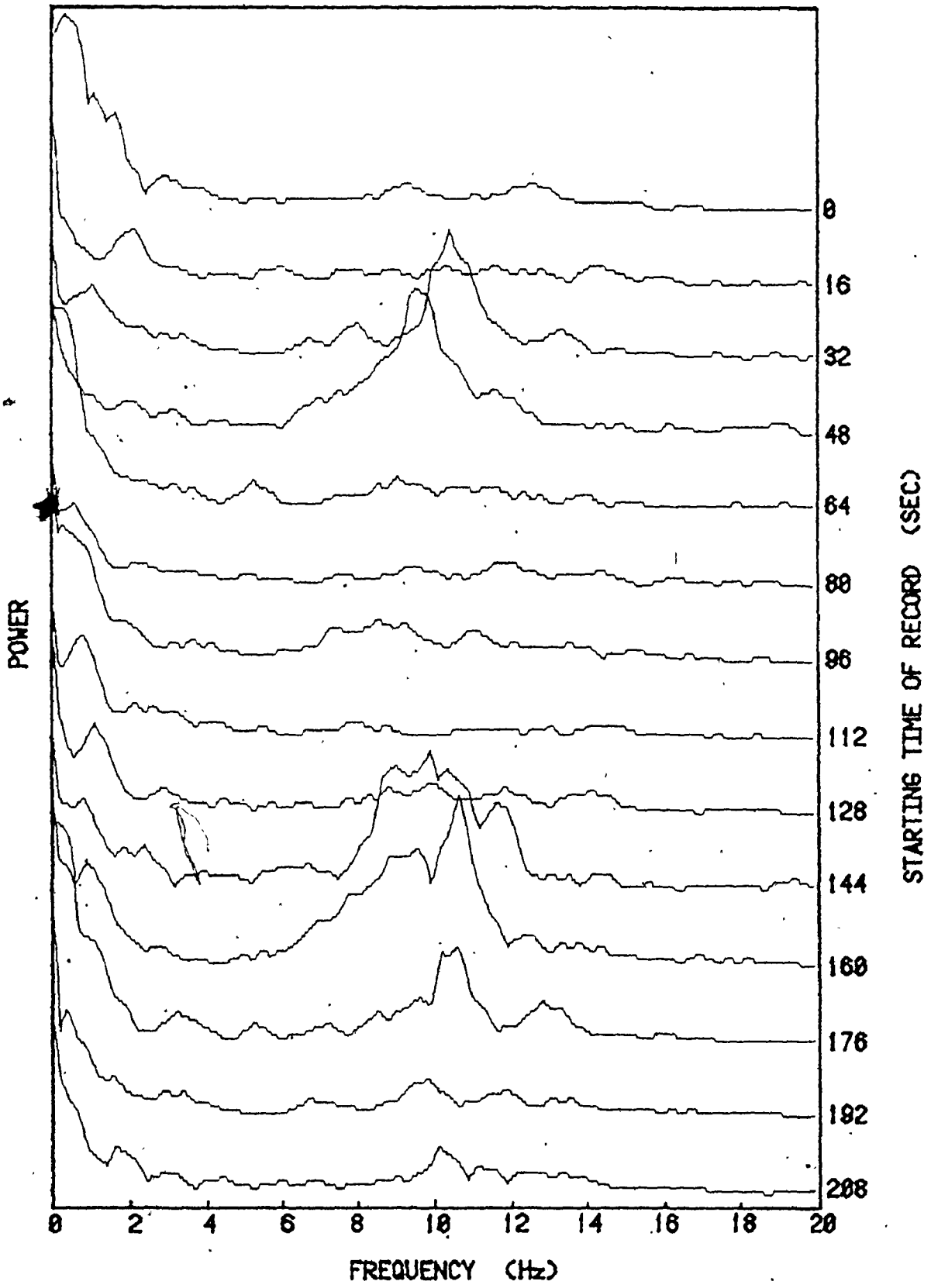

FIG. 3.7 SUM OF FOUR 4-SEC POWER SPECTRA

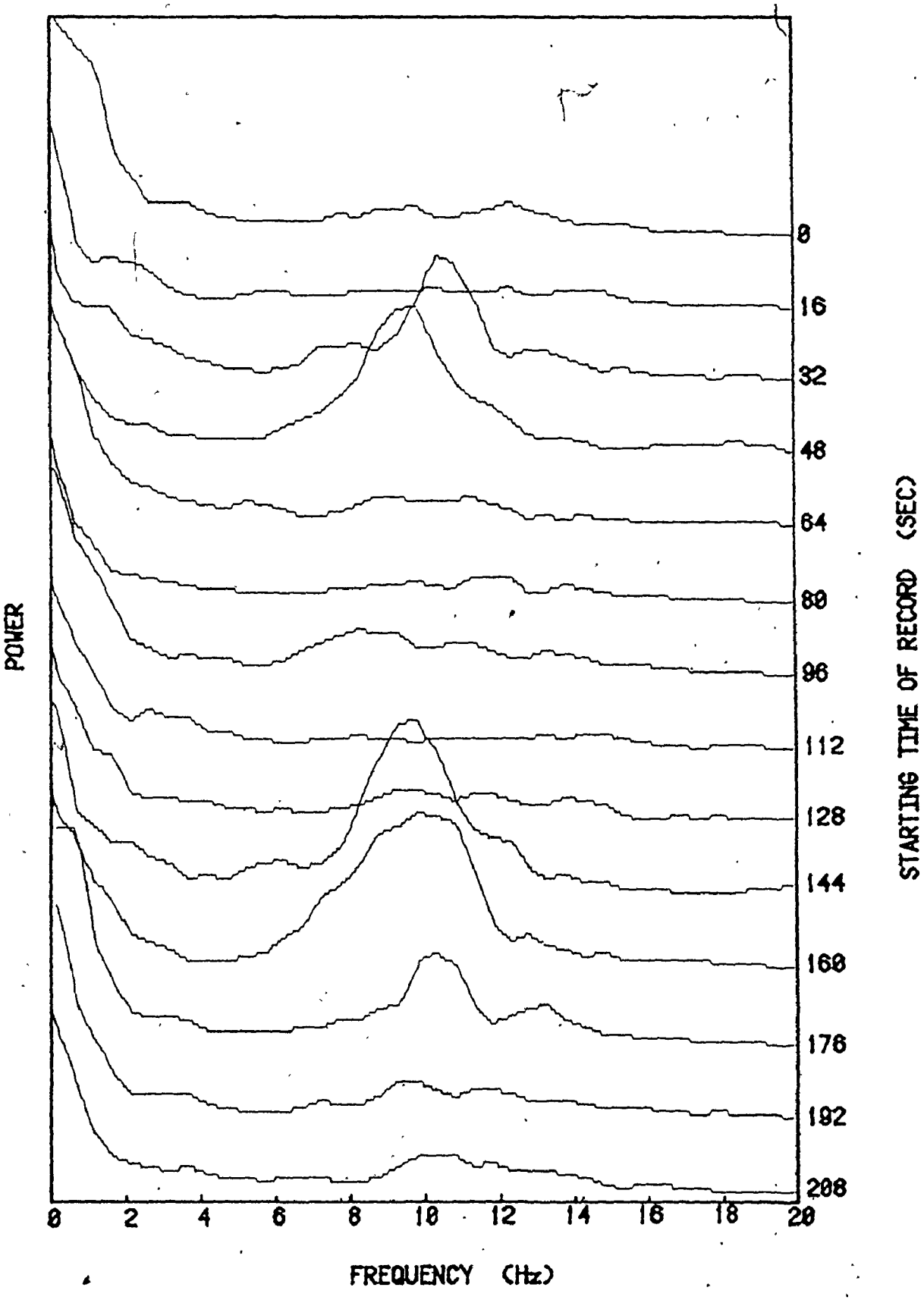

FIG. 3.8 SUM OF EIGHT 2-SEC POWER SPECTRA

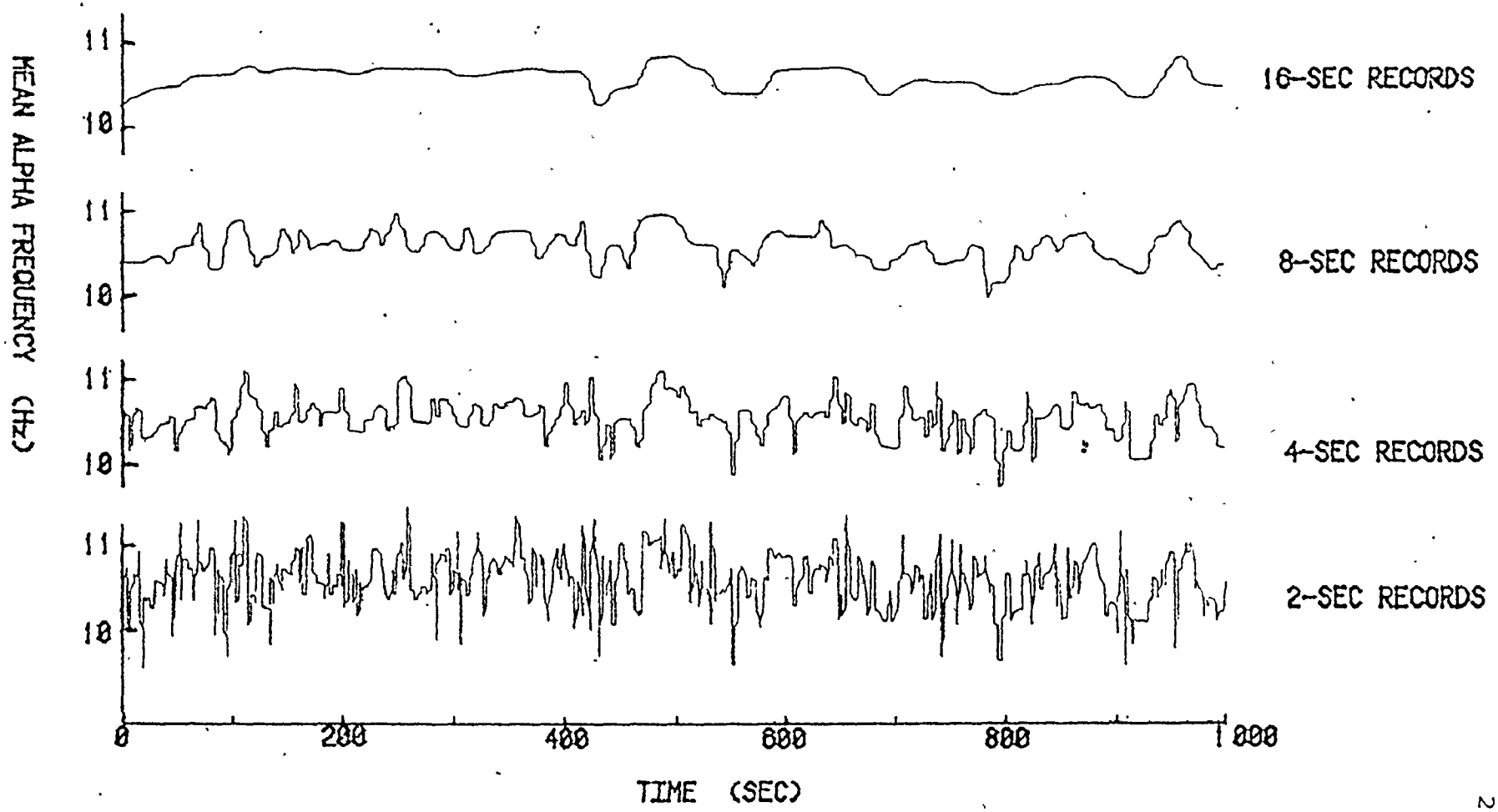

FIG. 3.9 VARIATION OF ALPHA FREQUENCY WITH TIME

series from specified functions followed by determination of the corresponding power spectra. Results drawn were slightly degraded by inaccuracies in the plotter. Nevertheless, the important features are still evident. Figure 3.10 shows the frequency spectrum of the basic 10-Hz sine function, followed by the effects of limiting the duration of the function with rectangular window functions. The spectrum of the 10-Hz sine function consists of a narrow peak centered about 10 Hz. When the sine function is multiplied by a rectangular window, 1-second wide, the spectrum becomes the convolution of the two separate spectra, resulting in a widening of the 10-Hz peak as shown. A narrower window creates an even wider peak in the frequency domain. Note that since the resulting spectrum is represented by the square of the sinc function, minor side peaks are present in the spectrum.

Figure 3.11 shows the effect of employing sinusoidal windows in an attempt to simulate alpha spindles. This results in a spectrum which has a wider peak and negligible side frequencies. In figure 3.12 simulated alpha bursts were placed at various positions within the record to show that all phase information is lost in power spectral analysis. In general, phase relationships are retained by the ratios of the amplitudes of the real and imaginary frequency components. Knowledge of these ratios is then lost when the power spectrum is computed from the sum of the squares of the two components. Also seen in figure 3.12 is the fact that the spectrum is un-

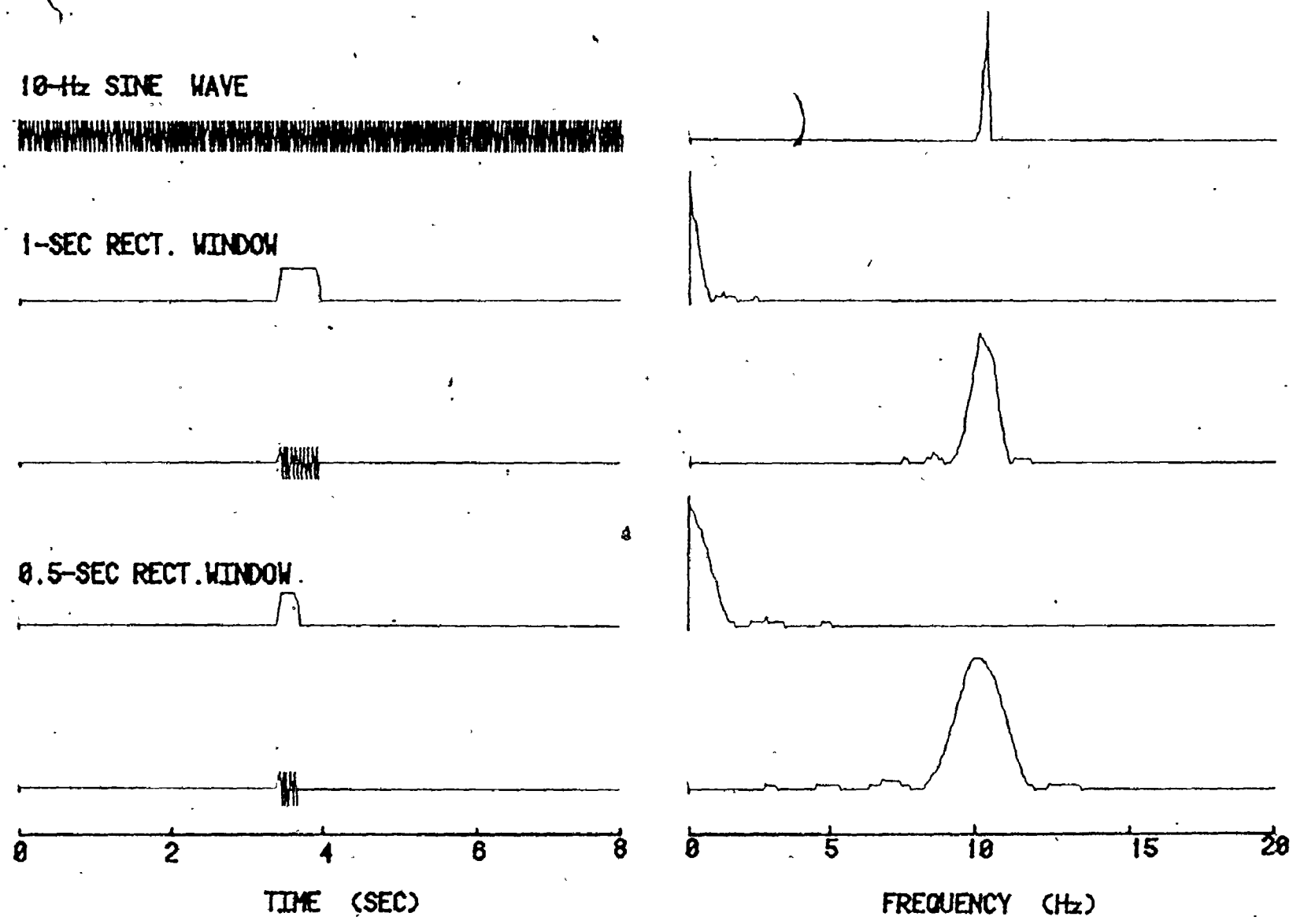

FIG. 3.10 POWER SPECTRA OF 10-Hz SINE WAVE WITH RECT. WINDOWS

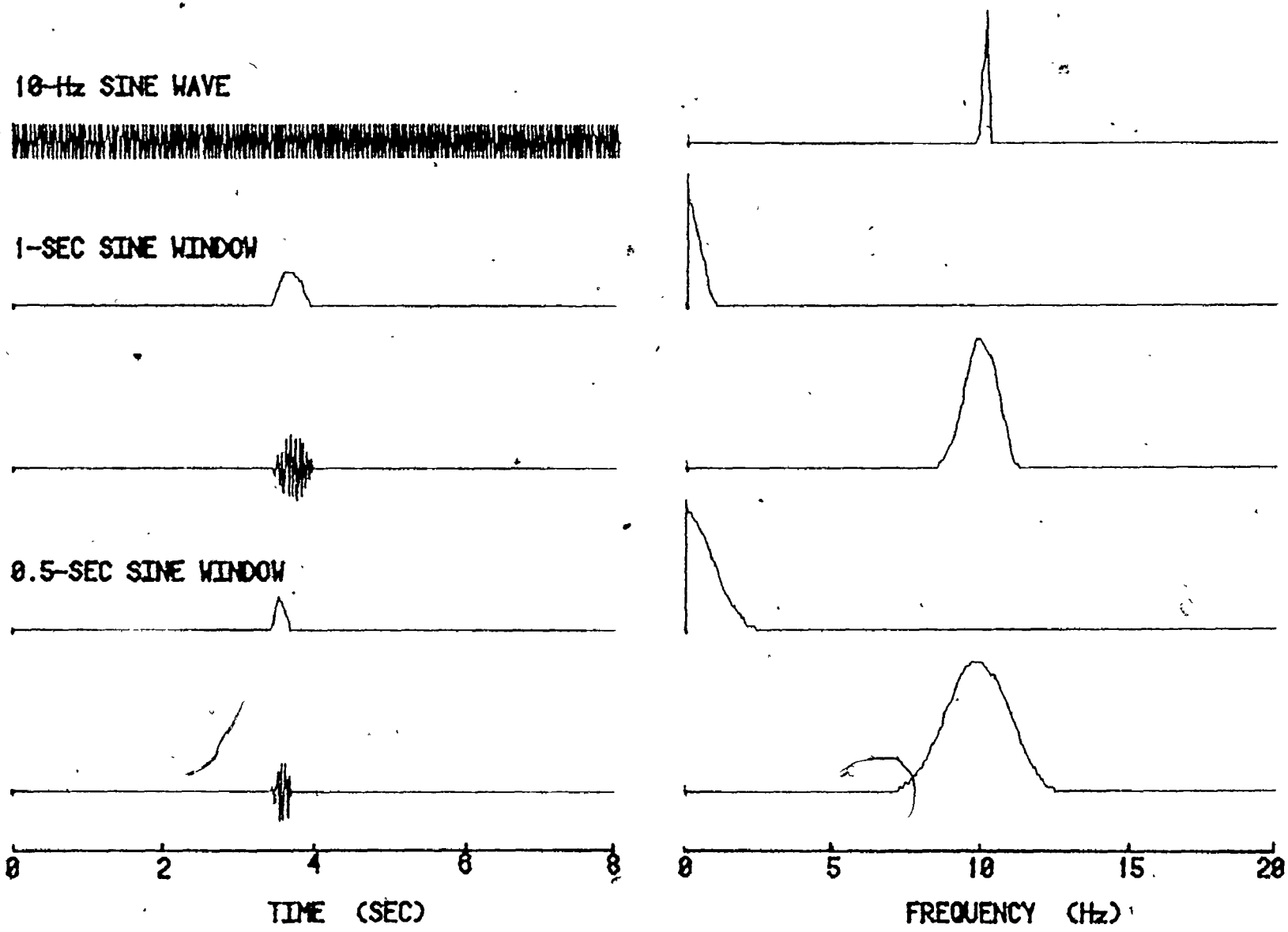

FIG. 3.11 POWER SPECTRA OF 10-Hz SINE WAVE WITH SINE WINDOWS

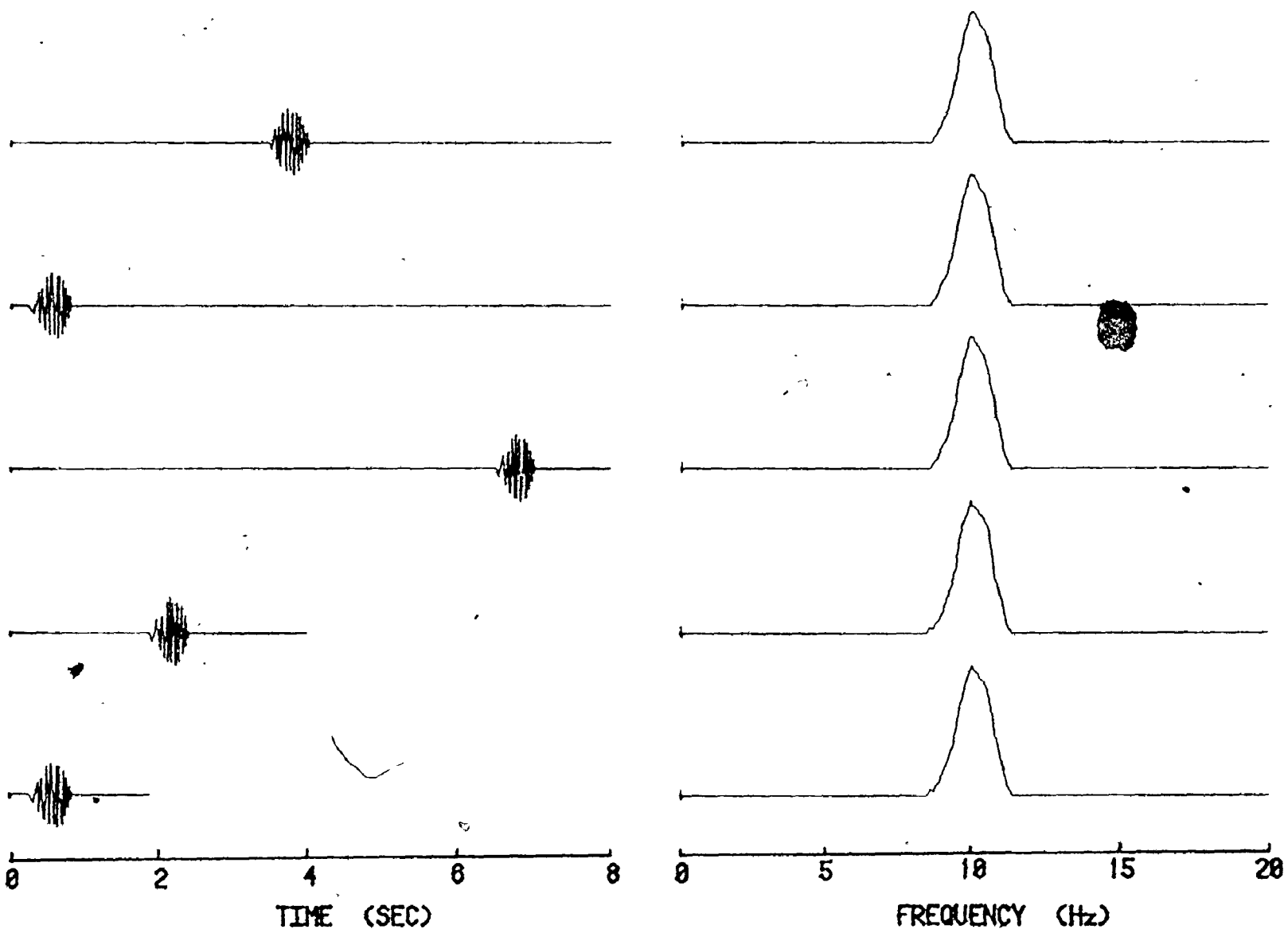

FIG. 3.12 POWER SPECTRA OF SIMULATED ALPHA SPINDLES AT VARIOUS POSITIONS WITHIN RECORDS OF DIFFERENT SIZE

affected by the array size of the time series. The results remain unchanged provided that the extent of the time record is enough to contain the entire alpha spindle.

Two interesting features are displayed in figures 3.13 and 3.14. In the former, when two identical spindles were positioned at different times apart, multiple peaks were created in the frequency domain. These results can be interpreted empirically from experience with the FT. Centering of the spectrum about 10 Hz arises from the basic 10-Hz content of the time series. The bell-shaped envelope is the result of the 1-second duration of the spindles. The pair of spindles can be considered to have resulted from a single spindle convolved with a pair of impulse functions. Since the FT of a pair of impulse functions is a cosine function the net result consists of a cosine function multiplied by the FT of a single spindle. This effect is clearly seen in figure 3.13. The period of the cosine function is equal to one-half of the time interval between the two spindles.

Figure 3.14 shows the power spectrum of two spindles whose 10-Hz sine-wave contents differed in phase. The first spindle consisted of a 10-Hz sine function commencing with 0-degree phase angle while the second spindle began with phase angles from 0 to 270 degrees. The plots clearly indicate a dramatic change as the phase difference is varied. These results demonstrate that even though all phase information

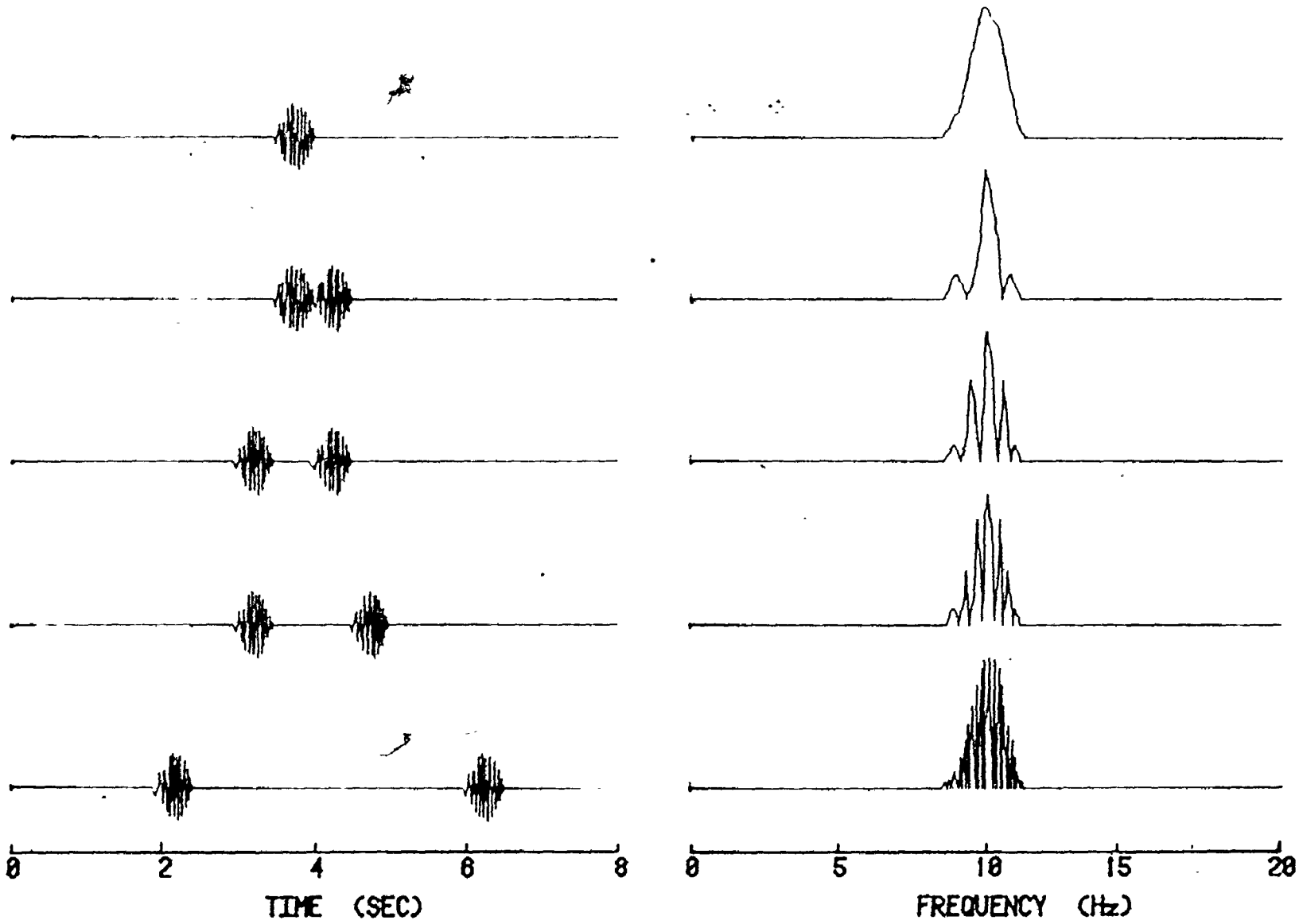

FIG. 3.13 POWER SPECTRA OF SIMULATED ALPHA SPINDLES AT VARIOUS POSITIONS IN TIME

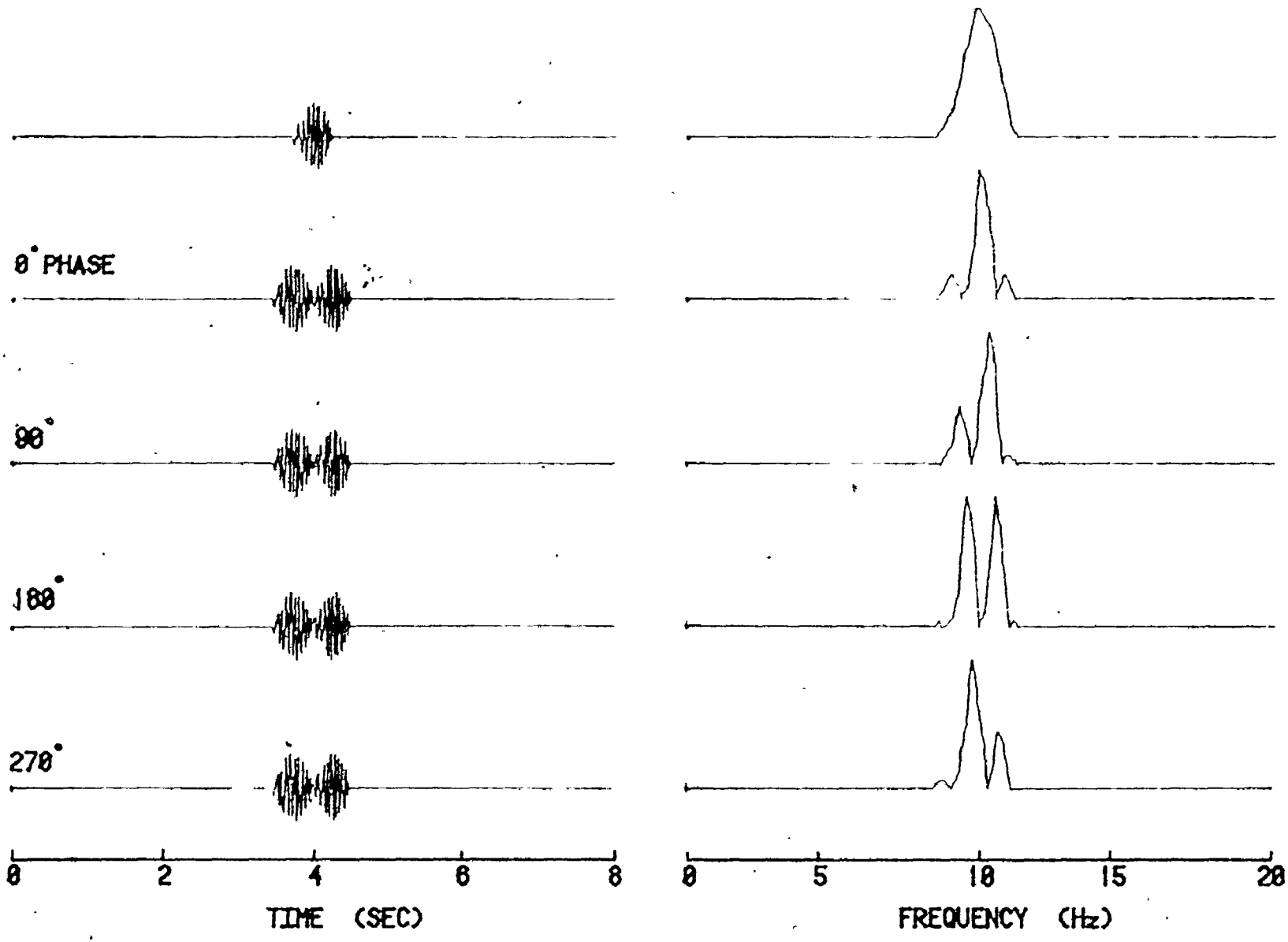

FIG. 3.14 POWER SPECTRA OF SIMULATED ALPHA SPINDLES UNDER VARIOUS CONDITIONS OF PHASE DIFFERENCE

is lost in the final power spectrum, phase differences certainly determine the structure of the spectrum.

It is now not difficult to appreciate, in terms of the last two effects, the great complexity of power spectra derived from EEG records. Figures 3.5 to 3.17 show that these effects do contribute to the overall structure of the spectra. A typical 8-second segment of an actual EEG record, along with its power-frequency spectrum, is shown in figure 3.15. This segment was then filtered using an idealized digital band-pass filter ranging from 8 to 13-Hz. The filtered signal is shown as the lower graph of figure 3.15. From this record, segments of alpha activity were selected and then transformed to show how drastically the spectrum becomes modified as different bursts are included. Note that the power spectra of real alpha spindles are not much different from those of the simulated spindles used previously. However, when a segment with two or more spindles are analyzed the net spectra shows no resemblance to the spectra of the individual spindles.

3.3 Discussion

The analysis clearly shows that the occurrence of many sharply defined peaks in the alpha region of the power spectra of an EGG record can be mainly attributed to (i) the shape of the amplitude envelope of the fundamental 10-Hz alpha wave

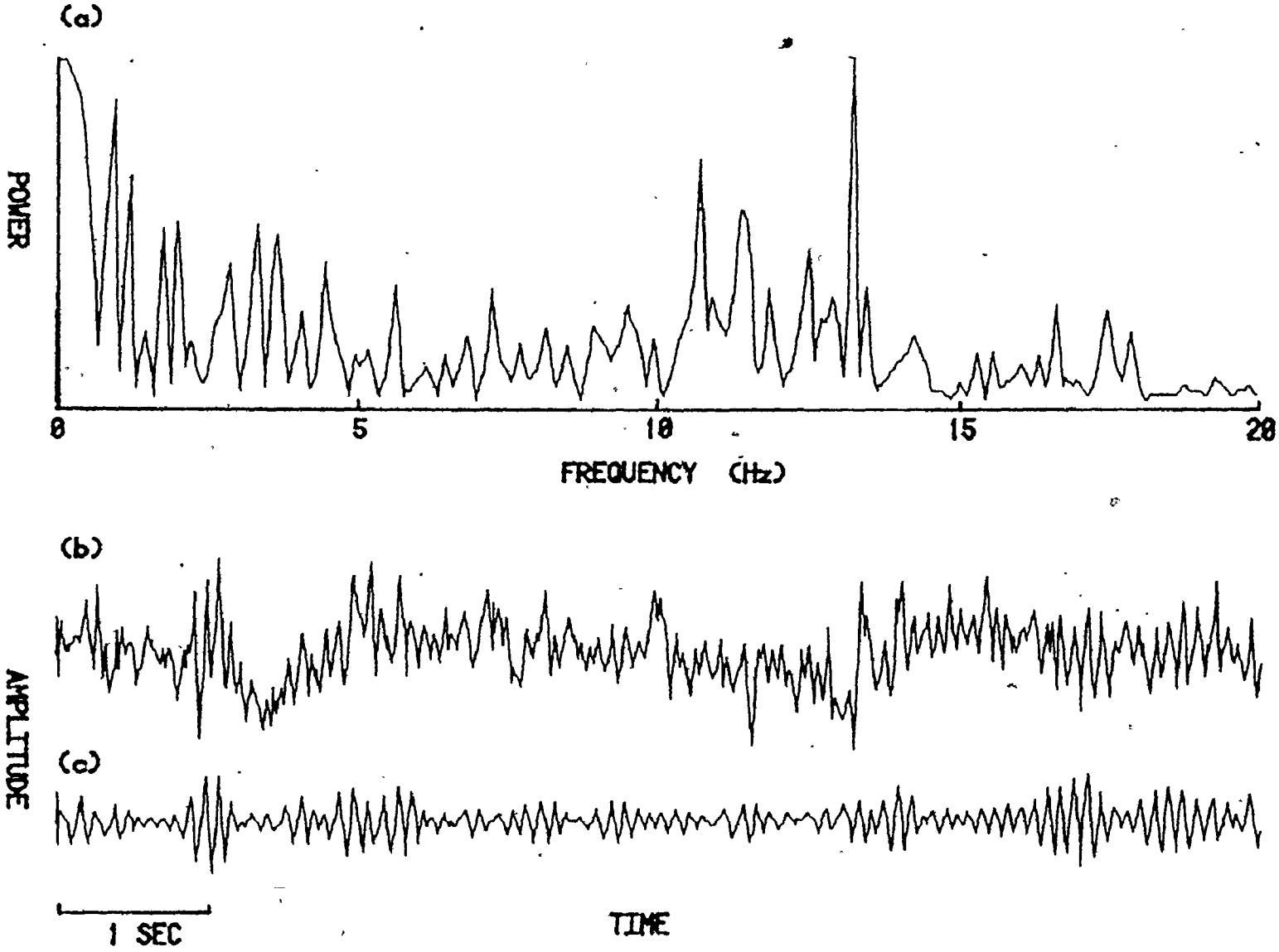

FIG. 3.15 (a) POWER SPECTRUM OF 8-SEC RECORD
(b) 8-SEC EEG RECORD (c) RECORD AFTER FILTER

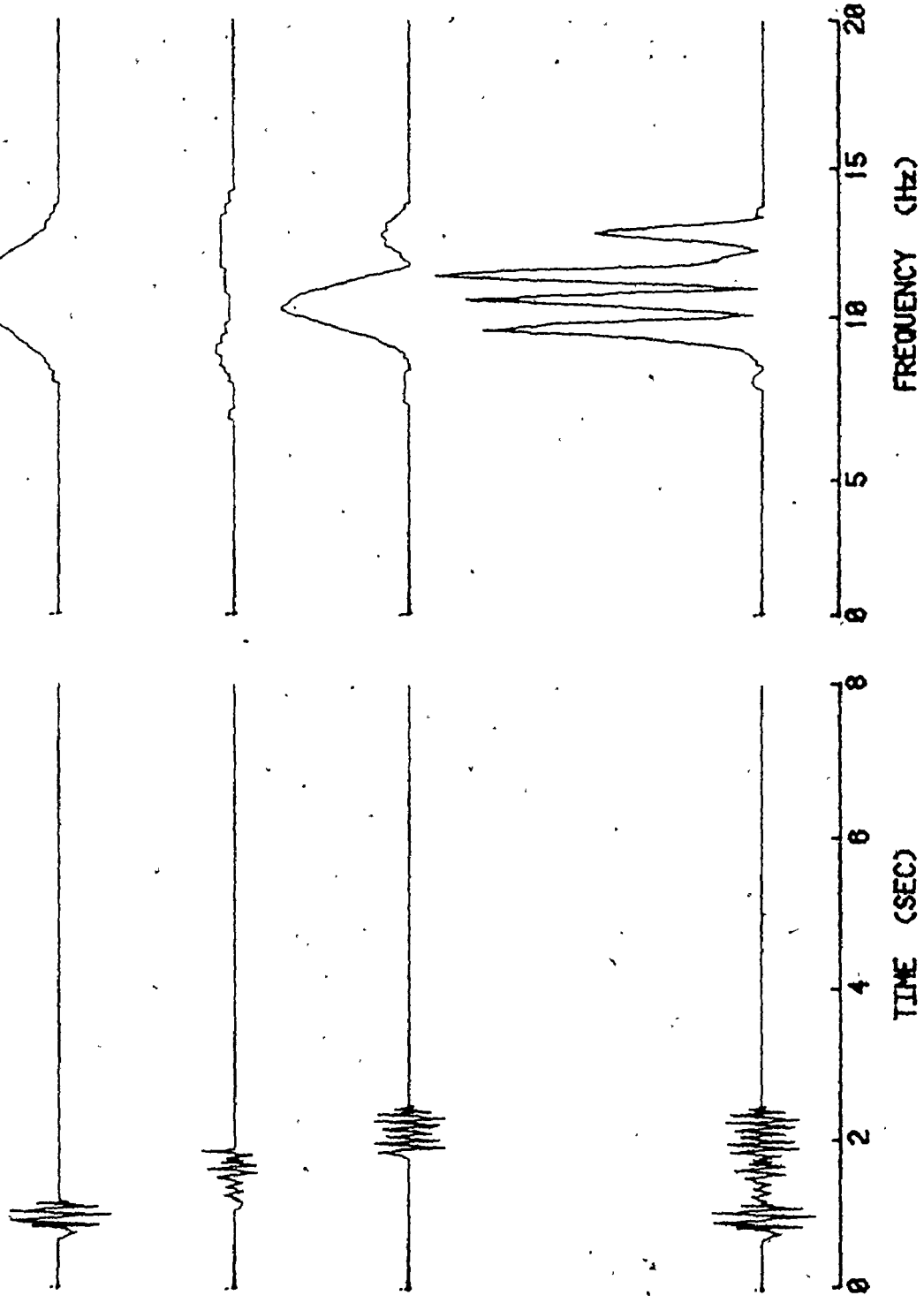

FIG. 3.16 POWER SPECTRA OF EEG SEGMENTS

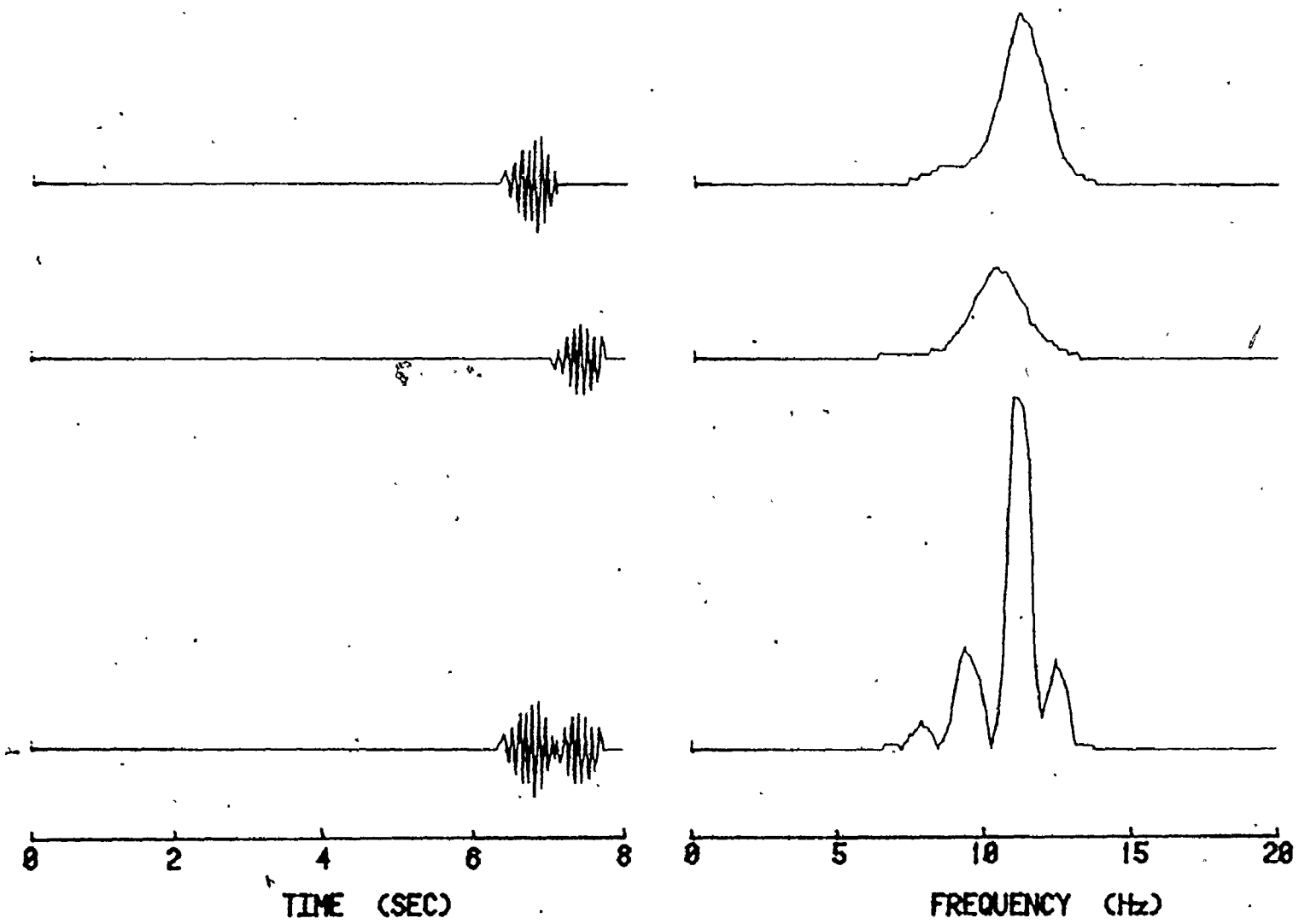

FIG. 3.17 POWER SPECTRA OF EEG SEGMENTS

and (ii) phase shifts within the 10-Hz alpha wave. When interpreting the power spectra of EEG as typically shown in figure 3.1, one can make the following general conclusions.

(i) The spread of spectral information about the 8 to 13-Hz region is not caused exclusively by alpha waves at these frequencies but is due also to the short duration of alpha spindles.

(ii) The existence of multiple peaks within this region is due to the combined effect of the random occurrence of alpha spindles and the phase relationship of the alpha waves which constitute the spindles.

(iii) The width of the multiple peaks is inversely related to the extent of the time record.

As a result of these observations a number of questions have arisen.

(i) Is it possible to determine a meaningful estimate of the mean alpha frequency from a typical power spectrum as shown in figure 3.15 or figure 3.16?

(ii) What significance should be attached to the determination of a mean alpha frequency when in fact there is no alpha activity present in the EEG segment?

(iii) How can the presence of alpha activity be ascertained?

(iv) What other methods are there of determining the mean alpha frequency?

It is hoped that at least some of these questions may be resolved by use of a spindle recognition mechanism based on amplitude and duration criteria.

CHAPTER 4

AMPLITUDE AND DURATION DISCRIMINATION

4.1 Implementation

In an effort to establish the presence of alpha activity, minimum threshold levels of spindle amplitude and duration were applied to the EEG. These processes were implemented in the form of computer analyses performed on previously stored EEG data. Figure 4.1 illustrates the first three steps of this procedure. Figure 4.1(a) represents an 8-second segment of a typical EEG recording. This segment was then filtered by an idealized digital band-pass filter, ranging from 8 to 13 Hz, to produce the result shown in figure 4.1(b). The filtered data was then squared, figure 4.1(c), and finally smoothed by means of a filter of 0.25-second time constant. This resulted in a curve, shown in figure 4.1(d), which represented the instantaneous power of the EEG record. This curve will be referred to as the power envelope. The purpose of creating the power envelope is to obtain a signal which relates to the absolute value of the EEG, and which will assist in the identification of spindles. Since the power envelope varies as the square of the amplitude of the EEG, the dynamic range in amplitude is expanded. It therefore becomes easier to dis-

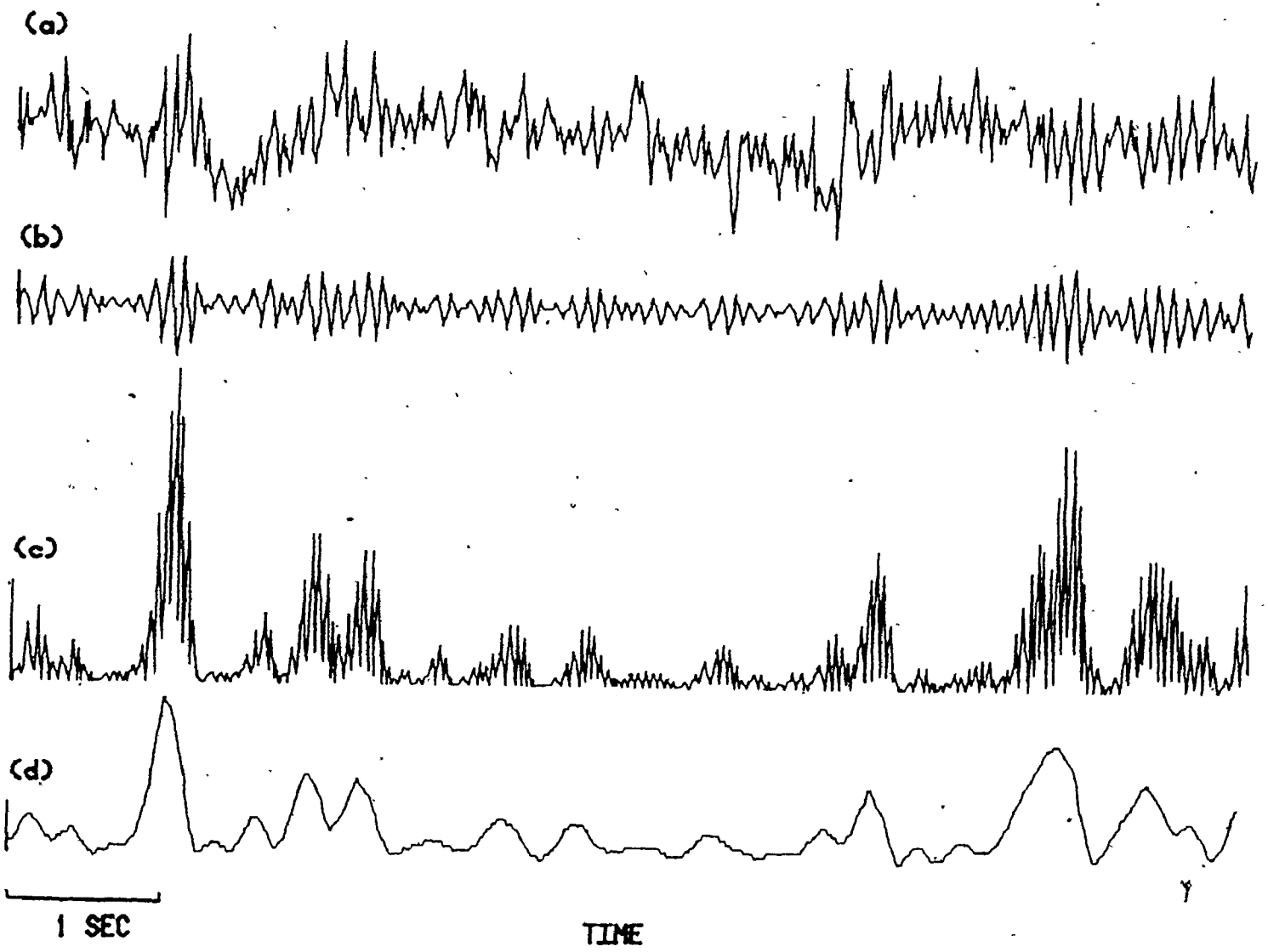

FIG. 4.1 (a) ORIGINAL EEG
(b) AFTER 8 TO 13-Hz FILTER
(c) SQUARE OF (b)
(d) POWER ENVELOPE

criminate against lower amplitudes associated with noise.

Before an amplitude threshold was applied, the distribution of the peak values of the power envelope were examined. Peaks were identified by making use of first and second differences. Zero values of the first differences indicated the presence of maxima or minima. Negative values of the second differences signified maxima. Peak values determined in this manner from the power envelope of a 640-second EEG record were ordered into bins to produce the result shown in figure 4.2. The arithmetic mean power occurred at the 0.1 level (arbitrary units) as shown on the graph. A power threshold at this level was selected, thus resulting in discrimination against any power peaks which fell below the mean power value.

Power discrimination at the selected threshold was then applied to the power envelope as illustrated in figure 4.3(b). Whenever the power envelope exceeded the threshold, EEG data was accepted. This produced segments of the EEG record as shown in figure 4.3(c). Application of duration criterion in effect determined the number of continuous waves which had to appear before the segment was accepted as an alpha spindle. Figure 4.4 shows the result from the previous figure when only bursts of duration longer than 0.25 seconds were analyzed. Each alpha spindle which satisfied the two criteria was isolated and the corresponding power spectrum was determined.

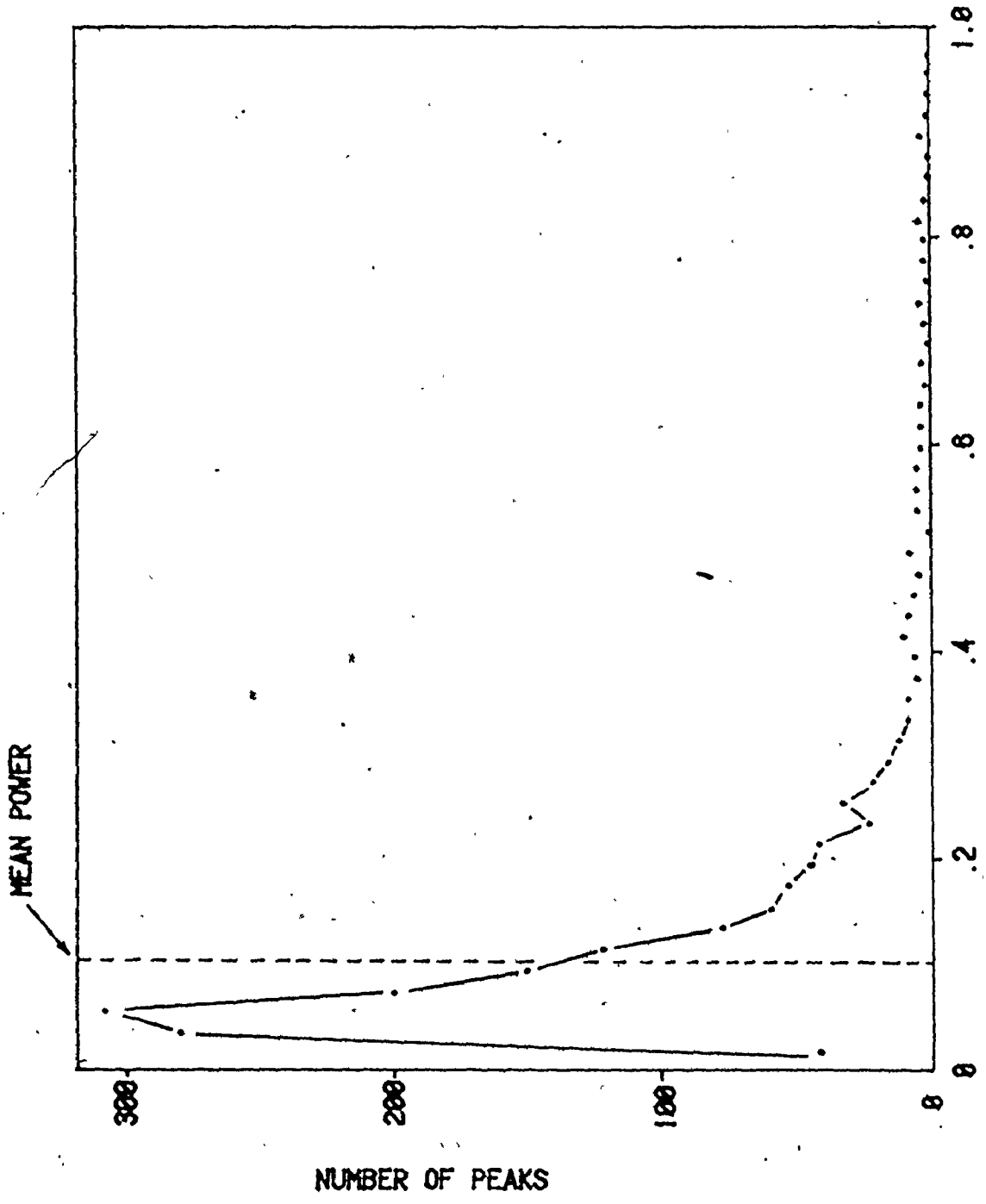

FIG. 4.2 DISTRIBUTION OF PEAK VALUES OF POWER ENVELOPE

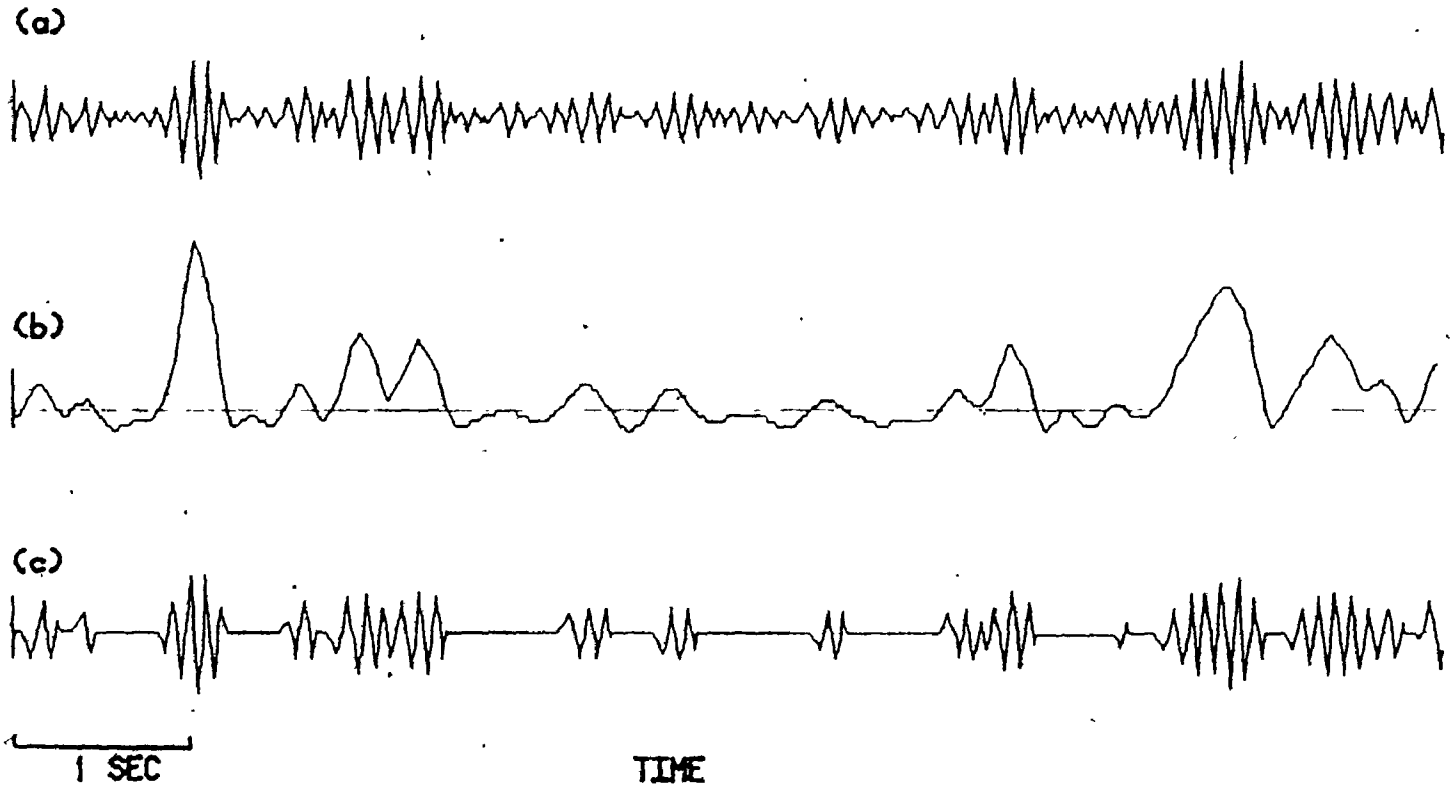

FIG. 4.3 APPLICATION OF POWER THRESHOLD

(a) FILTERED EEG RECORD

(b) POWER ENVELOPE WITH THRESHOLD SHOWN

(c) EEG SEGMENTS AFTER POWER DISCRIMINATION

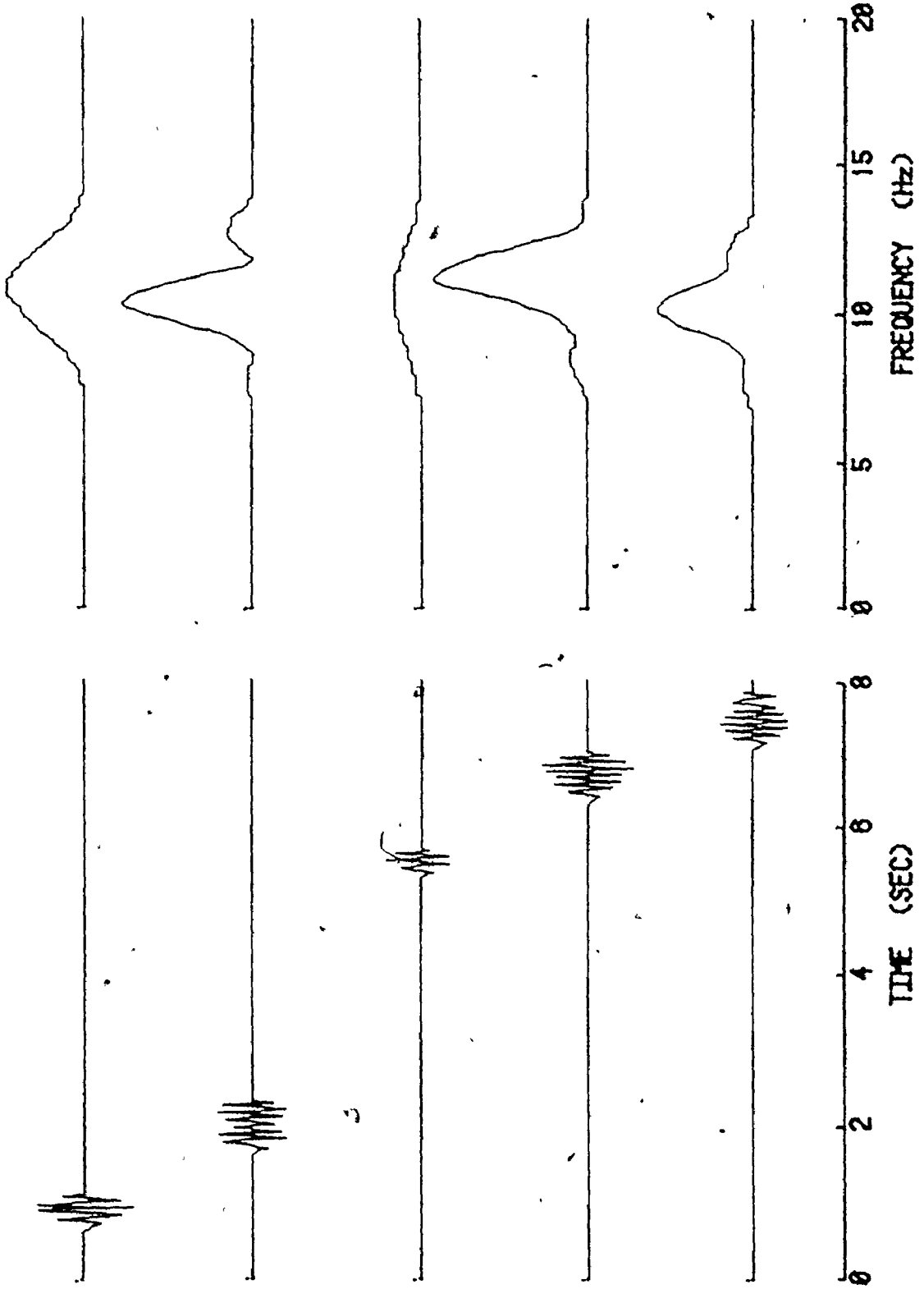

FIG. 4.4 APPLICATION OF POWER AND DURATION THRESHOLDS

4.2 Results

A 640-second EEG record was analyzed using a power threshold of 0.1 (arbitrary units) and duration threshold of 0.1 seconds. A sample of these results is shown in table 4.1. The first column, TIME, gives the time in seconds at which the alpha spindle appeared. MEAN ALPHA frequency was determined from the power spectrum by computing the mean value within the 8 to 13-Hz range. The ENERGY column shows the area occupied by an isolated peak of the power envelope and therefore represents the total energy of the alpha spindle. Zero-crossing (ZC) alpha is the alpha frequency determined by counting the number of times the signal crossed the zero-amplitude axis, while still satisfying the amplitude and duration criteria. The ZC-alpha can be computed as

$$\text{ZC-alpha} = \frac{\text{number of half cycles}}{2 \times \text{time interval between first and last crossings}} . \qquad (4\text{-}1)$$

However, since the time scale was quantized by a sampling rate of 64 Hz, the time interval was determined from the number of samplings within the first and last zero-crossings. Thus

$$\text{ZC-alpha} = \frac{\text{number of half cycles}}{\text{number of samplings}} \times 32 \text{ (Hz)}. \qquad (4\text{-}2)$$

Note that both the numerator and denominator are integers. This therefore results in the ZC-alpha having discrete values as can be seen in table 4.1.

TABLE 4.1 SPINDLE ANALYSIS FOLLOWING APPLICATION OF POWER AND DURATION THRESHOLDS

TIME (SEC)	DURATION (SEC)	MEAN ALPHA (HZ)	ENERGY (ARBITRARY)	ZC-ALPHA (HZ)
1.9	0.30	10.78	3.10	10.67
2.8	0.11	10.63	0.79	10.67
3.9	0.17	10.45	1.89	10.67
4.2	0.17	10.71	1.54	10.67
6.7	0.19	10.80	1.86	10.67
7.2	0.20	10.32	1.91	9.60
7.8	0.17	10.68	1.45	10.67
8.0	0.12	10.60	1.53	10.67
8.4	0.12	10.62	0.88	10.67
9.9	0.25	10.41	3.82	10.67
11.9	0.25	10.59	3.50	11.43
13.9	0.31	9.99	5.53	10.00
14.3	0.14	10.59	1.14	10.67
14.9	0.58	9.99	9.61	9.70
15.6	0.11	10.39	0.83	10.67
15.8	0.19	10.10	2.44	10.67
16.0	0.22	10.47	2.54	10.67
16.9	0.30	10.63	4.86	10.67
17.8	0.20	9.98	1.64	9.14
19.7	0.11	10.67	0.90	10.67
19.9	0.23	10.81	3.64	11.64
20.2	0.22	10.67	3.15	11.64
21.2	0.16	10.16	1.19	10.67
21.9	0.25	10.76	3.10	10.67
24.0	0.14	10.38	1.38	10.67
25.9	0.23	10.32	2.37	10.67
27.9	0.27	10.74	3.50	10.67
29.0	0.16	10.54	1.17	9.14
30.0	0.19	10.44	2.04	10.67
33.2	0.25	10.59	4.25	10.67
33.6	0.22	11.04	2.76	11.64
34.0	0.25	10.46	4.32	10.67
36.0	0.20	10.66	2.02	10.67
39.8	0.19	10.19	2.34	9.14
40.0	0.17	10.87	4.38	12.00
41.8	0.20	10.77	1.78	10.67
42.2	1.98	10.68	40.05	10.75

4.3 Statistical analysis of results

The results collected from the analysis of a 640-second EEG were examined in search for any important trends. Figure 4.5 shows the distribution of spindle energy, indicating that the number of spindles fell exponentially as energy increased. The distribution of the time interval between spindles is displayed in figure 4.6, with the same data drawn on a semi-log scale in figure 4.7. In general, events which occur at totally random intervals display an inverse-exponential distribution of time intervals. Thus the close linear fit apparent in figure 4.7 suggests that triggering of alpha spindles may be modelled as a random process.

Figure 4.8(a) shows the distribution of spindle duration along with the variation of mean alpha frequency and mean spindle energy. There appears to be a downward trend in the mean alpha frequency as spindle duration increases, figure 4.8(b). However, a linear least-squares fit which was performed on the data revealed that any such tendency could not be supported with a reasonable degree of confidence. This was mainly due to poor statistics resulting from a sample which was too small.

The data used in figure 4.8 are also shown in table 4.2. Mean alpha frequency, mean zero-crossing alpha frequency, and energy, together with their respective standard deviations are indicated for each group of spindles having a fixed

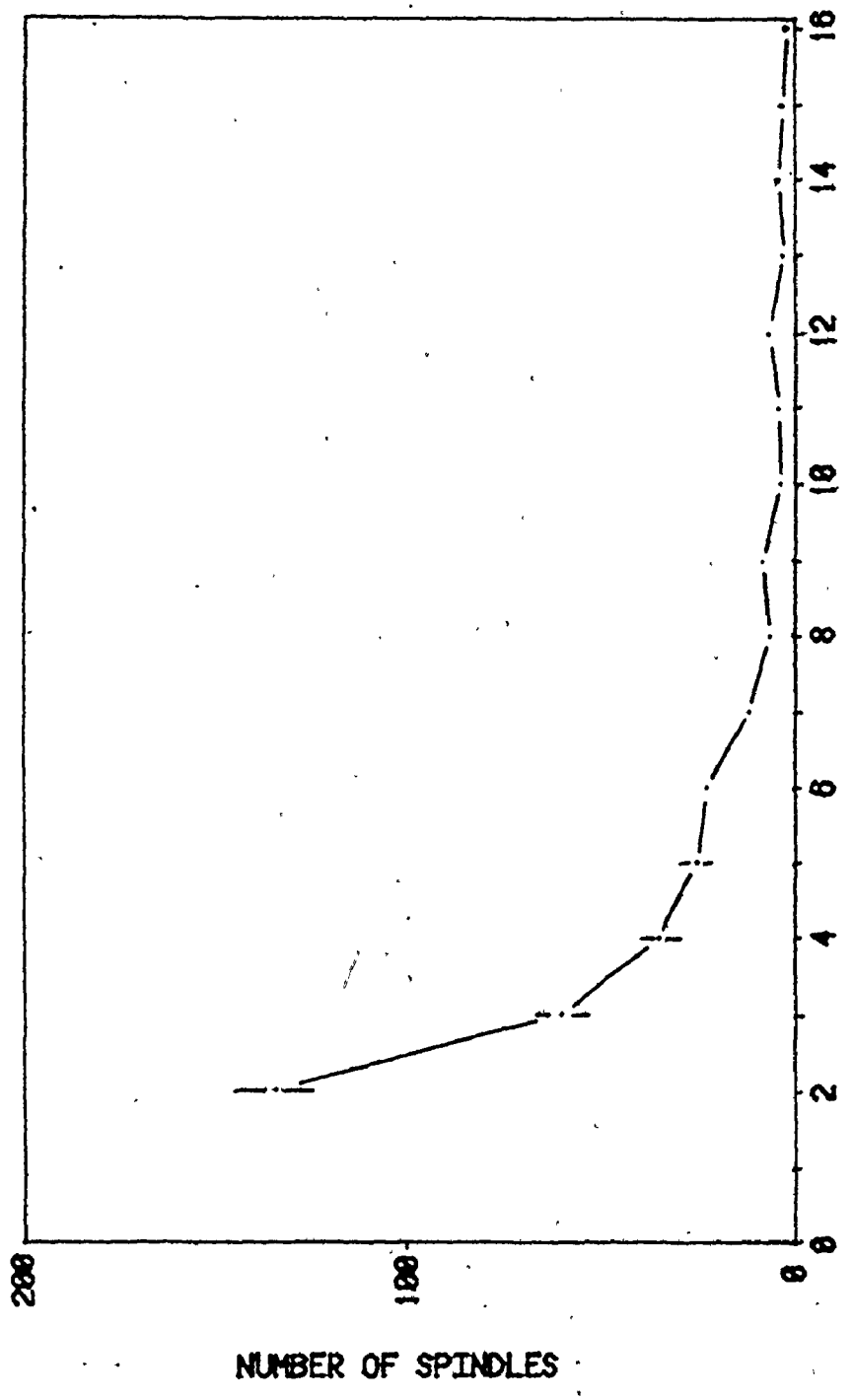

FIG. 4.5 DISTRIBUTION OF SPINDLE ENERGY

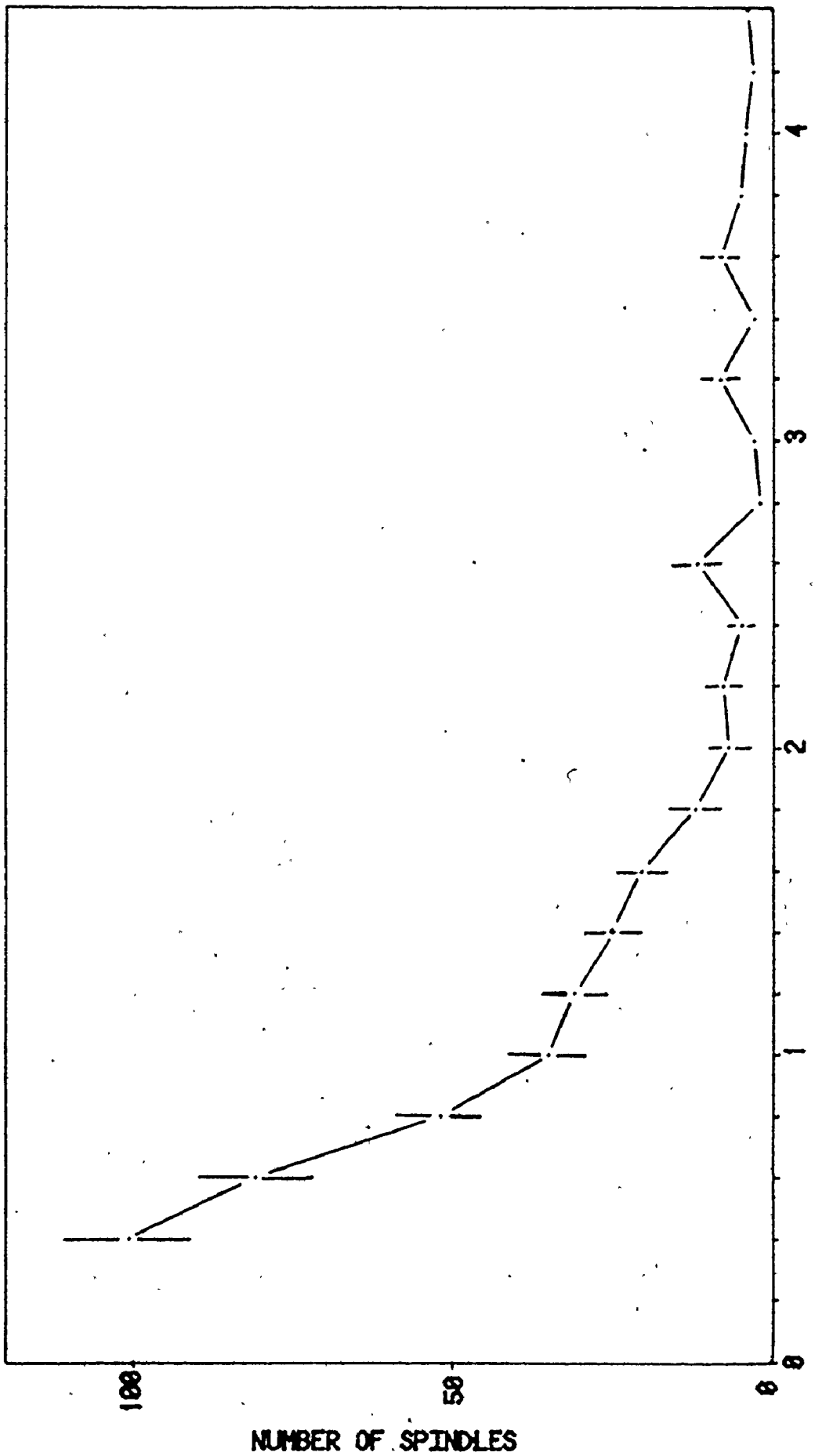

FIG. 4.6 DISTRIBUTION OF TIME INTERVAL BETWEEN SPINDLES

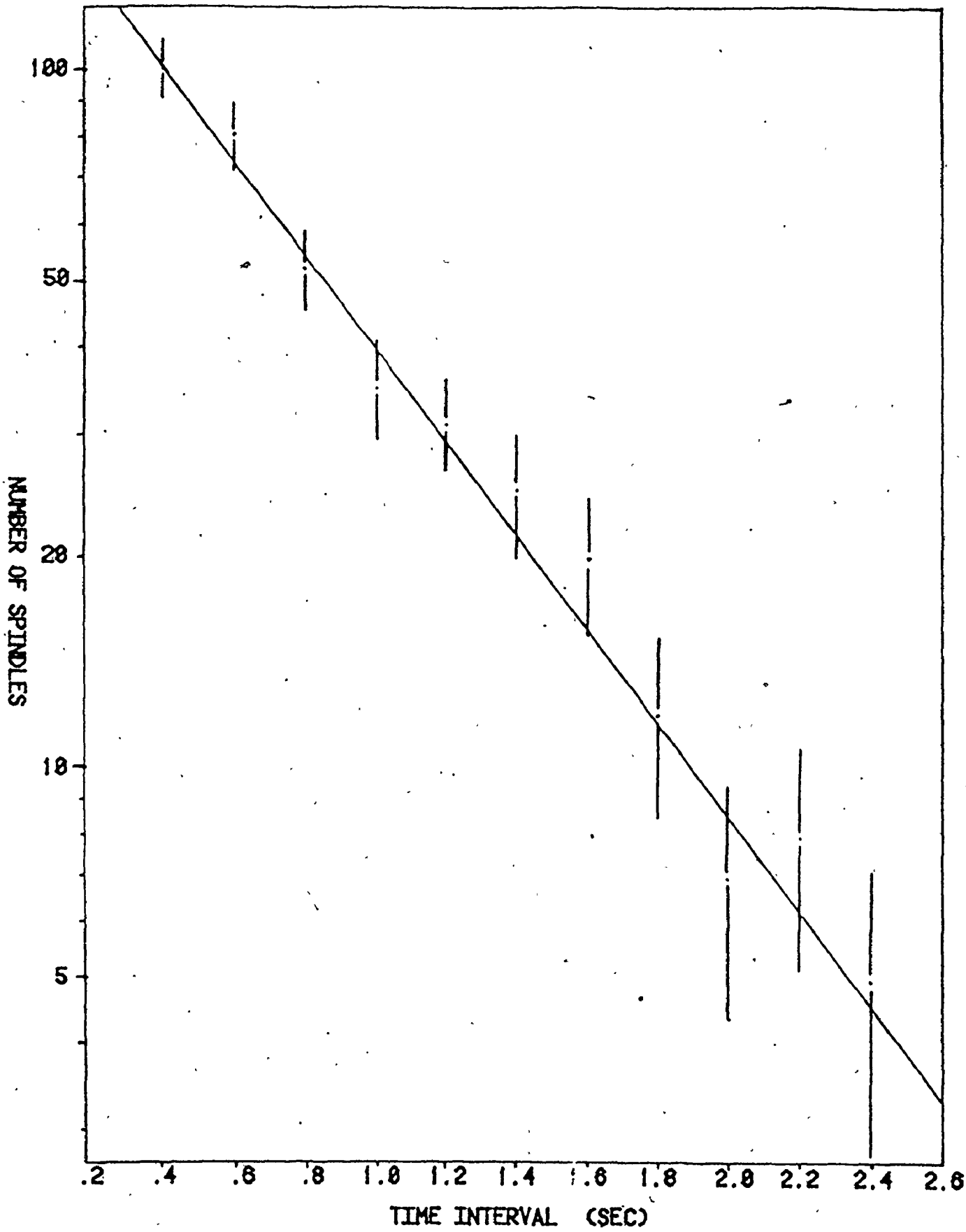

FIG. 4.7 DISTRIBUTION OF TIME INTERVAL BETWEEN SPINDLES

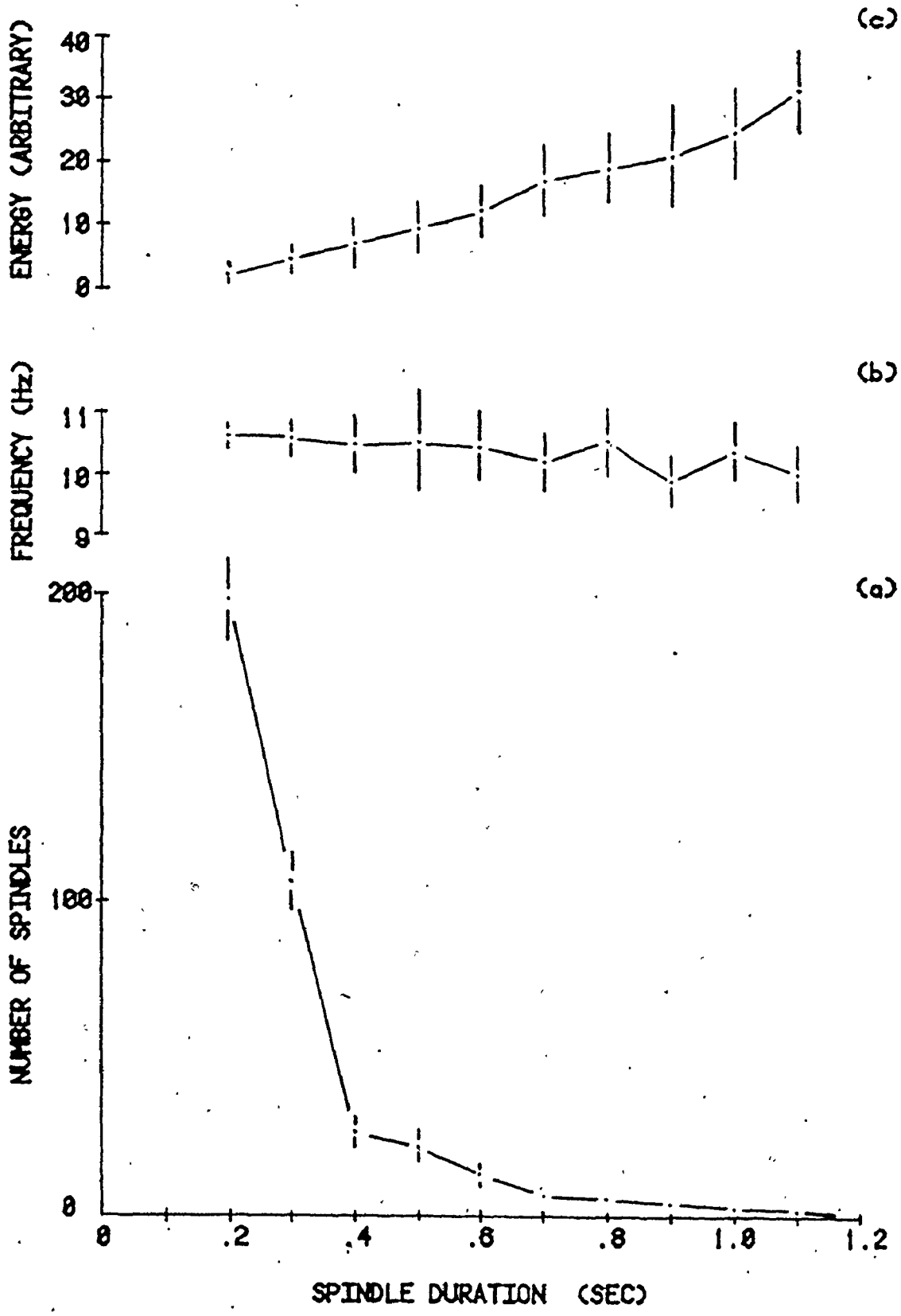

FIG. 4.8 (a) DISTRIBUTION OF SPINDLE DURATION
(b) MEAN ALPHA VS DURATION
(c) MEAN ENERGY VS DURATION

TABLE 4.2 STATISTICS OF SPINDLES GROUPED ACCORDING TO DURATION

DURATION (SEC)	COUNTS	MEAN ALPHA (HZ)	STD.DEV	Z/C ALPHA (HZ)	STD.DEV	CORR. COEF.	ENERGY (ARB.)	STD DEV
0.10	102.00	10.51	0.16	10.52	1.46	0.36	1.06	0.34
0.20	199.00	10.53	0.27	10.63	0.78	0.63	2.03	0.62
0.30	108.00	10.51	0.42	10.58	0.69	0.84	4.77	2.25
0.40	27.00	10.45	0.79	10.49	0.88	0.97	7.17	4.03
0.50	22.00	10.47	0.64	10.49	0.81	0.96	9.51	4.37
0.60	12.00	10.30	0.56	10.35	0.73	0.97	12.67	3.77
0.70	6.00	10.27	0.52	10.16	0.65	0.96	16.99	6.26
0.80	6.00	10.43	0.60	10.44	0.76	0.98	19.01	6.41
0.90	4.00	9.73	0.39	9.80	0.34	0.97	21.07	7.76
1.00	2.00	10.46	0.23	10.33	0.24	0.99	24.65	7.37

range of duration. Linear-correlation coefficients for the two types of alpha frequencies were determined. These coefficients indicate how well the variations in the ZC-alpha frequency agree with those of the mean alpha frequency. A value of unity implies perfect correlation whereas zero result shows no correlation whatsoever. The results show that the two alpha frequencies are in close agreement for spindles whose durations exceeded 0.4 seconds. This would therefore apply to spindles which were at least four cycles in length. It is probable that the lower values of the linear-correlation coefficient for shorter spindles were caused by round-off errors introduced by the discreteness of the ZC-alpha frequency as previously explained. This can be clarified by increasing the sampling rate, thus improving the accuracy to which time interval is determined.

Finally, the combination of a power threshold of 0.1 (arbitrary units) and a duration threshold of 0.4 seconds was applied to a new 640-second EEG record. A section of these results is shown in table 4.3. From this record a total of 65 spindles which satisfy the two criteria were detected and analyzed. The results show that Z-C alpha results do agree closely with mean alpha results. The overall mean values are given below.

TABLE 4.3 SPINDLE INFORMATION FOR POWER THRESHOLD = 0.1 DURATION THRESHOLD = 0.4

TIME (SEC)	DURATION (SEC)	MEAN ALPHA (HZ)	ENERGY (ARBITRARY)	ZC-ALPHA (HZ)
1.7	0.42	10.09	6.00	10.18
5.4	0.47	10.43	9.02	10.29
27.1	0.52	9.44	7.90	9.48
33.9	0.52	10.57	5.67	11.03
43.1	0.44	11.45	6.35	11.64
56.9	0.81	11.25	19.38	11.57
59.6	0.84	9.88	26.94	9.85
65.0	0.41	9.73	8.51	9.60
80.3	0.41	11.44	4.98	11.13
87.4	0.53	11.42	14.58	11.73
129.9	0.64	11.02	14.08	11.24
134.4	0.48	9.82	5.81	9.48
166.7	0.50	10.12	14.87	10.29
177.6	0.61	11.06	8.84	11.29
224.8	0.55	9.88	10.76	9.60
233.6	0.67	11.13	20.55	11.24
240.1	0.67	10.31	15.86	9.85
241.2	0.61	10.24	10.07	10.06
243.0	0.62	10.53	6.10	10.35
249.1	1.03	10.63	29.86	10.16
258.4	0.41	10.32	8.30	10.18
266.9	0.61	10.58	11.64	10.67
271.4	0.58	11.03	15.13	11.64
273.8	0.47	11.26	6.21	11.08
279.3	0.73	10.57	22.14	10.67
280.0	0.77	9.98	20.49	9.67
281.9	0.42	11.08	5.22	11.13
286.6	1.02	10.30	19.44	10.49
288.5	0.67	9.75	23.96	9.51
289.2	0.62	10.05	16.74	10.06
345.8	0.41	11.08	8.09	11.20
360.7	0.55	10.23	8.18	9.93
400.1	1.06	10.23	31.46	9.97
401.7	0.92	9.76	11.22	9.71
405.3	0.47	10.24	11.70	9.85
412.1	0.42	9.46	6.67	9.33
412.6	0.94	9.33	18.61	9.48

Mean alpha frequency = 10.36 Hz Stand. dev. = 0.63

Mean ZC-alpha frequency = 10.36 Hz Stand. dev. = 0.75

Linear-correlation coefficient = 0.96 .

The value of the correlation coefficient close to unity supports the close agreement between the two frequencies and suggests that zero-crossing analysis can be successfully applied to alpha frequency analysis.

4.4 Conclusions

The foregoing analysis illustrated the application of power and duration criteria for establishing the presence of alpha activity. This technique allowed individual alpha spindles to be isolated for analysis. Frequency spectra of spindles were determined by the DFT process and were used to calculate the mean frequency of the alpha spindles. Zero-crossing analysis was proposed as an alternative method over spectral analysis for determining the mean alpha frequency. This method was shown to produce results which were in very close agreement with those obtained from power spectral analysis. In addition, zero-crossing analysis can be performed using inexpensive electronic components and does not require the use of costly computer systems.

Statistical analysis of alpha spindles was limited somewhat by the small quantity of data. Naturally, this can be corrected by a more extensive study. For future research one may wish to compare natural variations with induced variations.

CHAPTER 5

ALPHA FREQUENCY MONITOR

Design recommendations

The design of an inexpensive alpha-rhythm monitor can now be presented. The overall design is based on two conclusions which have resulted from this study. Firstly, the need for some form of pattern recognition of the alpha rhythm has been demonstrated. A technique based on amplitude and duration discrimination has been successfully implemented and is therefore one of the recommendations used in the design. The second conclusion is that zero-crossing analysis is a suitable method of determining the mean frequency of alpha spindles. This technique also has been implemented and verified in the study.

The various processes which were used in the computer analysis are illustrated in figure 5.1. These processes are now reviewed with the purpose of showing how they are to be adopted in the design. The EEG signal was preconditioned by an 8 to 13-Hz band-pass filter to eliminate frequency components which occur outside of this range. The idealized filter used is characterized by its flat response in the pass region and an abrupt cut-off in the transition regions. For practical reasons a simpler filter would have to be adopted. Selecting

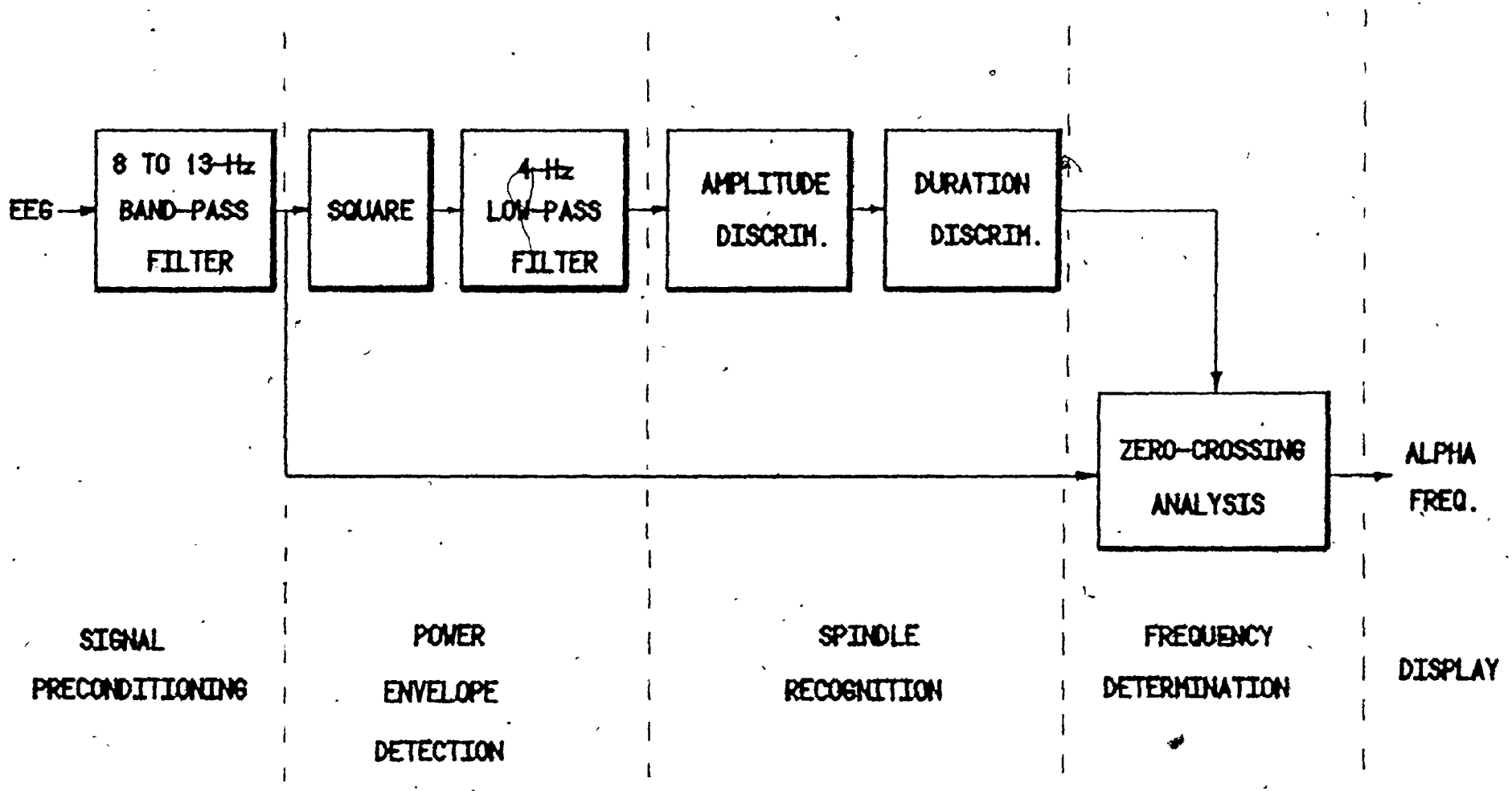

FIG. 5.1 BLOCK DIAGRAM OF PROPOSED MONITOR

a filter having the most appropriate response function may require some investigation. An excellent source of active-filter designs is therefore included in the reference[12].

The power envelope of the EEG is produced by the squaring function and 4-Hz low-pass filter. Various designs as well as ready-made circuits which perform an analog multiplication are available. Since the main function of the squaring circuit is to produce an absolute value of the EEG, this circuit may be replaced by a simpler full-wave rectification circuit. If this is done the system becomes less discriminating against non-alpha activity. The requirements of the 4-Hz low-pass filter are not stringent and a simple first-order filter should suffice.

Amplitude discrimination is most easily implemented by use of analog comparators. These techniques and circuits are widely known. Duration discrimination and zero-crossing analysis are two functions which may require some clever thinking. One possible design may make use of the output signal from the amplitude discriminator to dictate when the zero-crossing analyzer is to function. The output from the duration discriminator then determines if the result of zero-crossing analysis is acceptable. Whatever solution is arrived at, the design in this area requires some knowledge and experience in digital electronics. Nevertheless, the complexity and cost of this design should be minimal. It is beyond the scope of this study to attempt to solve this design problem.

Finally, the alpha frequency result can be displayed directly or may be recorded on a suitable medium for study at a later time. Features such as maximum and minimum frequency limiters, and audible or visible alarms may be incorporated as required. Implementation of these features should not present any problems.

APPENDIX A

FOURIER TRANSFORMS

The purpose of this appendix is to demonstrate through the use of illustrated examples some properties of the DFT which relate to power spectral analysis of the EEG. This is not intended to be a comprehensive treatise on the DFT. For more information the reader may wish to consult the literature given in the references[13,14].

The Fourier transform X(f) of the function x(t) is defined as

$$X(f) = \int_{-\infty}^{+\infty} x(t)e^{-i2\pi ft}\,dt \,. \qquad (A.1)$$

The inverse transform is given as

$$x(t) = \int_{-\infty}^{+\infty} X(f)e^{i2\pi ft}\,df \,. \qquad (A.2)$$

The two functions x(t) and X(f) are called Fourier transform pairs. When continuous time signals are sampled for digital processing the FT is approximated by the Discrete Fourier transform (DFT). The DFT pair then becomes

$$X(f) = \frac{1}{N} \sum_{t=0}^{N-1} x(t) e^{-i2\pi ft/N} \qquad (A.3)$$

$$x(t) = \sum_{f=0}^{N-1} X(f) e^{i2\pi ft/N} . \qquad (A.4)$$

The fast Fourier transform (FFT) is an efficient algorithm for computing the DFT. The frequency-domain function X(f) is, in general, complex. The power spectral density function p(f) represents the distribution of power along the frequency axis and can be calculated as

$$p(f) = |X(f)|^2 . \qquad (A.5)$$

This function is therefore always real and positive.

Convolution theorem

The convolution of two functions g(t) and h(t) is defined as

$$g(t)*h(t) = \int_{-\infty}^{+\infty} g(\tau)h(t-\tau)d\tau . \qquad (A.6)$$

The convolution theorem can be represented as

$$g(t)*h(t) = G(f)H(f) \qquad (A.7)$$

and conversely as

$$G(f)*H(f) = g(t)h(t) \qquad (A.8)$$

where G(f) and H(f) are the Fourier transforms of g(t) and

h(t) respectively. Thus a multiplication in one domain is represented as a convolution in the other domain.

Examples

Figure A.1 illustrates the use of the convolution theorem when two time signals are multiplied. Figure A.1(a) shows the FT of a infinite, continuous cosine function. The result is represented by a pair of impulse functions that are symmetric about zero frequency. Figure A.1(b) shows a rectangular window function along with its Fourier transform. When the cosine function is multiplied by the window function, a cosine function of finite duration is produced as shown in figure A.1(c). This multiplication in time domain is equivalent to convolution in frequency domain. Thus the FT of the product of the time functions is the convolution of the individual transforms. This result is shown in figure A.1(c) where the pair of impulse functions takes on the shape of the transform of the window function.

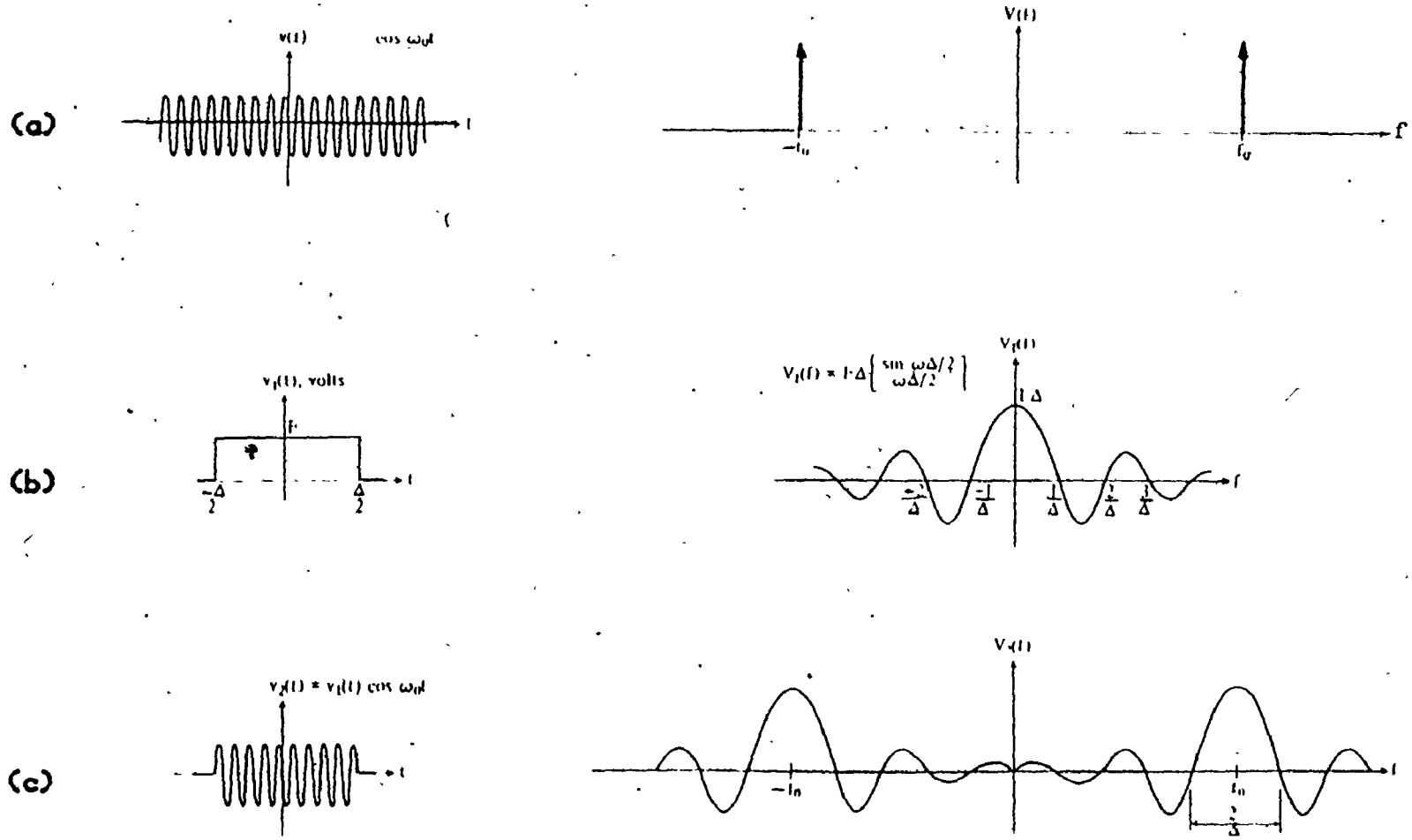

FIG. A.1 EXAMPLES OF FOURIER TRANSFORMS AND CONVOLUTION
(a) COSINE FUNCTION
(b) RECTANGULAR WINDOW FUNCTION
(c) COSINE MULTIPLIED BY WINDOW FUNCTION

REFERENCES

(1) M.A.B. Brazier, (Ed.), "Computer techniques in EEG Analysis". Electroenceph. Clin. Neurophysiol., Suppl. 20, (1961).

(2) D.O. Walter and M.A.B. Brazier, "Advances in EEG Analysis". Electroenceph. Clin. Neurophysiol., Suppl. 27, (1968).

(3) M. Fink, T.M. Itil and D.M. Shapiro, "Digital Computer Analysis of the Human EEG in Psychiatric Research". Comprehens. Psychiat., 8:521-538, (1967).

(4) L.G. Kiloh, A.J. McComas and J.W. Osselton, "Clinical Electroencephalography", Butterworths, London, (1972).

(5) F.A. Gibbs, D. Williams and E.L. Gibbs, "Modification of the Cortical Frequency Spectrum by Changes in CO_2, Blood Sugar, and O_2". J. Neurophysiol., 3:49-57, (1940).

(6) J.W. Cooley and J.W. Tukey, "An Algorithm for the Machine Calculation of Complex Fourier Series". Math. Comput., 19:297-301, (1965).

(7) D.O. Walter, J.M. Rhodes, D. Brown and W.R. Adey, "Comprehensive spectral analysis of human EEG generators in posterior cerebral regions". Electroenceph. Clin. Neurophysiol., 20:224-237, (1966).

(8) S. Giaquinto and F. Marciano, "Automatic Stimulation Triggered by EEG Spindles". Electroenceph. Clin. Neurophysiol., 30:151-154, (1971).

(9) J.R. Smith, W.F. Funke, W.C. Yeo and R.A. Ambuehl, "Detection of Human Sleep EEG Waveforms". Electroenceph. Clin. Neurophysiol., 38:435-437, (1975).

(10) N.R. Burch, W.J. Nettleton, J. Sweeney and R.J. Edwards, "Period analysis of the Electroencephalogram on a general-purpose digital computer". Ann. N.Y. Acad. Sci., 115:827-843, (1964).

(11) M.W. Johns, E.B. Stear and J. Hanley, "Tracking the dominant frequency of the EEG by phase-locked loop demodulation", Electroenceph. Clin. Neurophysiol., 37:414-416, (1974).

(12) D. Lancaster, "Active-Filter Cookbook". Sams, Indiana, (1976).

(13) G.D. Bergland, "A guided tour of the fast Fourier transform". IEEE Spectrum, 6:41-52, July (1969).

(14) R. Bracewell, "The Fourier Transform and its Applications", McGraw-Hill, New York, (1965).